universität wien

MASTERARBEIT / MASTER'S THESIS

Titel der Masterarbeit / Title of the Master's Thesis

„Dynamics of the Yang-Mills field on the Einstein universe“

verfasst von / submitted by

Magnus von Terzi, BSc

angestrebter akademischer Grad / in partial fulfilment of the requirements for the degree of

Master of Science (MSc)

Wien, 2023 / Vienna, 2023

Studienkennzahl lt. Studienblatt / degree programme code as it appears on the student record sheet:	UA 066 876
Studienrichtung lt. Studienblatt / degree programme as it appears on the student record sheet:	Masterstudium Physics
Betreut von / Supervisor:	Assoz. Prof. Dr. David Miro Fajman

Abstract

We consider the Yang-Mills field propagating on the Einstein universe and study the long-time behaviour of small solutions. Due to the resonant character of the linearised spectrum and the lack of dissipation of energy, this model displays interesting dynamical phenomena, while being conformally related to the four-dimensional Anti-de Sitter spacetime.

Using the method of multiple-scale analysis, we construct the resonant system, which accurately approximates the original equation. This infinite dimensional dynamical system manifests remarkable properties, such as a three-dimensional invariant manifold. We generalise the analysis of [1] and find non-trivial time-periodic solutions with exact energy return to the initial data and a variety of stationary states (without energy transfer between modes). Furthermore we investigate the turbulent behaviour of solutions with three-mode and generic initial data numerically.

Zusammenfassung

Wir betrachten das Yang-Mills Feld, welches sich auf dem Einstein Universum ausbreitet und studieren das Langzeitverhalten von kleinen Lösungen. Aufgrund des resonanten Charakters des linearisierten Spektrums und dem Mangel von Dissipation von Energie, zeigt dieses Modell interessante dynamische Phänomene, während es konform verwandt ist mit der vier-dimensionalen Anti-de Sitter Raumzeit.

Mithilfe der Methode der Mehrskalenanalyse konstruieren wir ein resonantes System, welches die ursprüngliche Gleichung genau approximiert. Dieses unendlich dimensionale dynamische System manifestiert bemerkenswerte Eigenschaften, wie etwa eine drei-dimensionale invariante Mannigfaltigkeit. Wir verallgemeinern die Analyse von [1] und finden nicht-triviale zeitperiodische Lösungen mit exakten Energie Rücklauf zu den Anfangsdaten und eine Vielfalt an stationären Lösungen (ohne Energietransfer zwischen den Moden). Desweiteren untersuchen wir das turbulente Verhalten von Lösungen mit drei-Moden und generischen Anfangsdaten numerisch.

Acknowledgements

I would like to thank my supervisor Dr. Maciej Maliborski, for suggesting this topic, his continuous and frequent support and allowing me to present this topic at CERS13 in Stockholm. Moreover, I would like to thank Prof. Fajman and the Gravitational physics group of the University of Vienna for their hospitality and respectful attitude towards me.

Finally I thank Alisha and my family for their advice and aid to get me also through the stressful and difficult times.

Contents

Chapter 1

Introduction

In this thesis we are studying the dynamics of the Yang-Mills field on the Einstein universe. This model can be seen as a toy model to help us understand the instability of Anti-de Sitter (AdS) spacetime. Anti-de Sitter is a maximally symmetric spacetime with a negative cosmological constant. As for the other two maximally symmetric spacetimes (Minkowski, de Sitter) with zero and positive cosmological constant, stability has been proven by [2] for Minkowski and [3] for de-Sitter. The difference between these spacetimes is, that in Anti-de Sitter spacetimes energy cannot dissipate towards infinity for a reflective boundary. Numerical and analytic studies indicate that AdS is in fact unstable against black hole formation for a large class of arbitrarily small perturbations and reflective boundary conditions [4, 5, 6]. In [7] it was shown that for the same model, which was used to conjecture the instability of AdS [4], time-periodic solutions can be constructed. In contrast, non-trivial time-periodic solutions do not exist for asymptotically flat spaces [8, 9].

Asymptotically AdS spacetimes also gained a lot of attention from the AdS/CFT correspondence. This duality connects the dynamics of AdS to dynamics of a certain quantum conformal field theory in one spatial dimension less. Collapse to a black hole corresponds to the process of equilibration and thermalization [10]. The class of small perturbations of AdS that do not form a black hole translates to dynamical CFT configurations that do not equilibrate [11].

For the instability of AdS two features are essential: The existence of a reflective boundary that acts as a mirror and prevents energy from dissipating and a fully resonant spectrum of linear perturbations of AdS. The first condition is not exclusive to AdS as shown in [12], by considering a spherically symmetric self-gravitating scalar field enclosed in a timelike worldtube with reflecting boundary conditions. The numerical simulation indicates that arbitrarily small perturbations evolve into a black hole. We therefore expand our perspective and also study the long time behaviour of nonlinear waves on spatially confined domains.

An essential simplification to the nonlinear dynamical equations is the resonant approximation [11, 13]. Other names are renormalisation method [14], time averaging [15], effective equation [16] or multi-scale analysis [17]. This simplification is obtained by rewriting the nonlinear dynamical system using linearised normal modes. These equations then contain rapidly oscillating terms. Most of these terms can be discarded when considering small perturbations. The remaining terms determine the evolution on long-time scales and correspond to the interactions between the modes. An advantage of the resonant system is that it approximates the dynamics at small ε (size of perturbation). The resonant system is invariant under scaling, so only one simulation is required to display the dynamics for the entire range of sufficiently small epsilon [13].

Because of the complexity of the resonant dynamics of AdS, in particular the complexity of the interaction coefficients [13, 14, 15], it makes sense to search for simpler related systems [5, 6, 18]. These 'toy models' show interesting non-trivial dynamical behaviour. One can also study designed mathematical systems that have an identical structure to the resonant system coming from AdS dynamics [19, 20, 21]. Resonant systems derived from AdS-related studies [22, 5, 18, 23] all indicate the same pattern: They possess exact solutions parameterised by an

invariant submanifold and the dynamics on this manifold show exactly periodic energy transfer of the initial state. In [1] these resonant systems are categorized and it is shown that this very large class of solvable cubic resonant systems admits an extra conserved complex-valued quantity.

In this thesis we study the dynamics of the resonant system of the Yang-Mills field on the Einstein universe and extend the work of [24]. After reviewing the research on Anti-de Sitter instability in Chapter 2, we repeat basic definitions of general relativity and give an introduction to AdS spacetime and the Einstein universe in Chapter 3. In Chapter 4 we derive the equations of motion for the Yang-Mills field on the Einstein universe and study linear perturbations of the static solution. The derivation of the resonant system for this model is in Chapter 5 and its conserved quantities are given in Chapter 6. In Chapter 7 we compare the resonant system to the PDE solution and show that it approximates the nonlinear dynamics sufficiently. Finally in Chapter 8, we study the dynamics of the resonant system analytically and numerically.

Chapter 2

Review of the instability of Anti-de Sitter

AdS is a ground state among asymptotically AdS spacetimes (spacetimes with the same conformal boundary as AdS) due to the positive energy theorem [25]. Hence one naturally asks the question about the stability for that state, i.e. do small perturbations close to the static solution remain small for all times. For Minkowski, which is a ground state for asymptotically flat spacetimes [26], the question has been answered by the famous paper of Christodoulou and Klainerman [2] by proving that Minkowski is globally stable, see also the more recent work [27, 28, 29]. In the de Sitter case, Friedrich has proved global stability for $3+1$ dimensions [3], which was extended to all even dimensions, c.f. [30].

The difference between asymptotically Minkowski or de Sitter spacetimes and asymptotically Anti-de Sitter spacetimes is the timelike boundary at conformal infinity, where boundary conditions need to be prescribed. This makes the question of stability for Anti-de Sitter more challenging and still unproven. In 1982 Breitenloher and Friedmann showed linear stability of Anti-de Sitter [31], which was extended and completed more recently by Ishibashi and Wald [32]. Despite of the extensive research on asymptotically Anti-de Sitter spaces since the AdS/CFT duality conjecture by Maldacena [10], the question of nonlinear instability of AdS space has mostly been ignored until 2011. A few exceptions are Friedrich [33], Ishibashi and Wald [32] and Anderson [34]. In the latter the author expects AdS space to be "dynamically stable, with the behavior of the nonlinear exact solutions nearby to g_{AdS} well-modeled on the linearized behavior."

In 2011, Bizoń and Rostworowski conjectured that AdS is unstable against black hole formation for arbitrarily small perturbations. Their study on a self gravitating spherically symmetric massless-scalar field in $3+1$ dimensions with negative cosmological constant, showed instability at time $\mathcal{O}(\varepsilon^{-2})$, where ε is the size of the perturbation [4]. This result was extended to AdS_{d+1} for $d \geq 3$ in [35]. Bizoń and Rostworowski stated two essential features. The first is the existence of a timelike boundary with reflective boundary condition, which acts as a mirror, such that energy cannot escape. The second condition is a resonant spectrum of the linear perturbation of AdS, which leads to weak turbulence, i.e. the shift of energy from low to high frequencies [4]. Their results also raised the question, if this turbulent behaviour is specific to asymptotically AdS spacetimes or can be found for other 'confined' models with reflective boundary conditions.In [12] Maliborski studied small perturbations of Minkowski inside a timelike worldtube $\mathbb{R} \times S^3$ and gave numerical evidence for instability. The author also answered the in [4] posed question about the role of the negative cosmological constant Λ, that is to create a timelike boundary [12]. In three dimensions, AdS is separated from the continuous black hole spectrum by a mass gap [36]. Small initial data has energy below this threshold, which makes it impossible for a black hole to form. In [37] they give numerical evidence that the evolution of small perturbations of AdS_3 remains globally smooth.

Since Bizoń and Rostworowski ignited the spark there has been extensive research to support their conjecture. For example Buchel and Lehner [38], who extended their analysis to complex scalar fields and reproduced the same phenomena as [4], or their studies on the stability of Boson stars in AdS [39]. In [40] the authors showed that for the purely gravitational problem, generic

initial perturbations lead to black hole formation. However they have also found, that if one starts with certain individual graviton modes, so called *geons*, the evolution is nonlinearily stable. These *geons* are the gravitational analogs to Boson stars [40]. The same authors came to the conclusion that the non-dispersive character of the linearised spectrum is necessary for instability [41]. The asymptotically resonant spectrum of *geons* [40] and Boson stars [39] is not strong enough to trigger instability (islands of stabilities). Maliborski and Rostworoski constructed time-periodic solutions for the model used in [4] in $d+1$ dimensions (for $d \geq 2$) [7].

In [11] the authors developed a new perturbative formalism, that is the *Two Time Framework*, and introduced resonant approximation to the studies of Anti-de Sitter instability. In agreement with the *Two Time Framework*, [14] resummed the secular terms in [4] using renormalization group method and analytically found explicit expressions for all the non-vanishing secular terms (extended in [15]). The resonant approximation was then applied to the system of [4] to show the development of an oscillatory singularity [13]. In [42], studying spherically symmetric Einstein-massless scalar fields in four to nine dimension, numerical methods have shown that the resonant systems introduced in [41] accurately approximate the full nonlinear theory well for dimension five to nine. In the case of four dimension the truncated system needs many more modes than in higher dimensions, to show the dynamics in a regime where a black hole forms. They conclude that although a lot of progress has been made in the conjecture of AdS instability, there is still a lot to do. The method from [15] has also been deployed to develop an infinite-dimensional *flow* system for the cubic wave equation in AdS_{d+1} [5]. Another *flow* system was constructed for the cubic wave equation on the Einstein cylinder, which is conformally related to the self-interacting conformally coupled scalar field in AdS. The constructed *conformal flow* then shows remarkable properties, such as a low-dimensional invariant subspace, a wealth of stationary states and solutions with non-trivial exactly periodic energy flows [22].

Most numerical simulations of AdS instability are restricted to spherical symmetry although there have been results without symmetry, that indicate instability of gravitational perturbations [40] (see also their follow up work [43, 44]). In [6] a different approach to the purely gravitational problem was applied. Using the cohomogeneity-two biaxial Bianchi IX ansatz they obtained a simple $1+1$ dimensional setup for AdS_5 and found a similar instability phenomena as in [4]. Another numerical evidence of gravitationally collapse away from spherical symmetry was by [45, 46], also for AdS_5.

A different more recent approach was by Moschidis, who proved the instability of Einstein-null dust system system first with an inner mirror [47] and the AdS instability conjecture for an Einstein-massless Vlasov system [48]. The work by Moschidis [48] encourages to an analytic understanding of Anti-de Sitter instability and that the conjecture is provable [42].

Chapter 3

Preliminaries

In this chapter we give preliminaries from general relativity and an overview of Anti-de Sitter spacetime and the static Einstein universe.

3.1 General Relativity

We state basic definitions from general relativity, relevant for the subsequent derivations, based on [49]. Let us therefore consider a Lorentzian metric

$$g = g_{\mu\nu}\mathrm{d}x^\mu \mathrm{d}x^\nu \,, \tag{3.1}$$

with signature $(-,+,+,+)$. We define the covariant derivative of a two-tensor $T^{\mu\nu}$ as

$$\nabla_\alpha T^{\mu\nu} = \partial_\alpha T^{\mu\nu} + \Gamma^\mu_{\beta\alpha} T^{\beta\nu} + \Gamma^\nu_{\beta\alpha} T^{\mu\beta} \,, \tag{3.2}$$

where the Christoffel symbols $\Gamma^\mu_{\beta\alpha}$ can be calculated through

$$\Gamma^\alpha_{\beta\gamma} = \frac{1}{2} g^{\alpha\beta} \left(\partial_\beta g_{\sigma\gamma} + \partial_\gamma g_{\sigma\beta} - \partial_\sigma g_{\beta\gamma} \right) . \tag{3.3}$$

Alternatively the Christoffel symbols $\Gamma^\mu_{\alpha\beta}$ can also be computed using the Lagrangian

$$\mathcal{L}(x^\mu, \dot{x}^\nu) = \frac{1}{2} g_{\alpha\beta}(x^\mu) \dot{x}^\alpha \dot{x}^\beta \,, \tag{3.4}$$

where $\dot{} \equiv \mathrm{d}/\mathrm{d}s$ denotes the differentiation with respect to the parameter s of a geodesic $s \mapsto \gamma(s)$. The Euler-Lagrange equations

$$\frac{\mathrm{d}}{\mathrm{d}s} \left(\frac{\partial \mathcal{L}}{\partial \dot{x}^\mu} \right) = \frac{\partial \mathcal{L}}{\partial x^\mu} \,, \tag{3.5}$$

yields the geodesic equation

$$\frac{\mathrm{d}^2 x^\mu}{\mathrm{d}s^2} + \Gamma^\mu_{\alpha\beta} \frac{\mathrm{d}x^\alpha}{ds} \frac{\mathrm{d}x^\beta}{ds} = 0 \,. \tag{3.6}$$

The Christoffel symbols $\Gamma^\mu_{\alpha\beta}$ can then be identified as coefficients of the first derivative terms. The curvature tensor for a vector field X^μ is given by

$$R^\mu_{\nu\rho\sigma} X^\nu = \nabla_\rho \nabla_\sigma X^\mu - \nabla_\sigma \nabla_\rho X^\mu \,, \tag{3.7}$$

which in local coordinates can be written as

$$R^\mu_{\nu\rho\sigma} = \partial_\rho \Gamma^\mu_{\sigma\nu} - \partial_\sigma \Gamma^\mu_{\rho\nu} + \Gamma^\mu_{\rho\alpha} \Gamma^\alpha_{\sigma\nu} - \Gamma^\mu_{\sigma\alpha} \Gamma^\alpha_{\rho\nu} \,. \tag{3.8}$$

3.2 Anti-de Sitter spacetime

We recall some basic facts and results from [50] and [51]. Anti-de Sitter is a solution to the vacuum Einstein equations

$$R_{\mu\nu} - \frac{1}{2}Rg_{\mu\nu} + \Lambda g_{\mu\nu} = 0\,. \tag{3.9}$$

with cosmological constant $\Lambda < 0$. It is the unique maximally symmetric Lorentzian manifold with negative constant scalar curvature.

We can define AdS_{d+1} as the hyperboloid

$$X_1^2 + ... + X_d^2 - U^2 - V^2 = l^2\,, \tag{3.10}$$

of radius l, determined by the cosmological constant $\Lambda = -\frac{d(d-1)}{2l^2}$ (c.f. [35]), embedded in a $d+2$ dimensional flat space with the metric

$$\mathrm{d}s^2 = \mathrm{d}X_1^2 + ... + \mathrm{d}X_d^2 - \mathrm{d}U^2 - \mathrm{d}V^2\,. \tag{3.11}$$

Through the parametrisation

$$X = r\omega, \quad (\omega \in \mathbb{S}^{d-1})\,, \tag{3.12}$$

$$U = \sqrt{r^2 + l^2}\sin\tau/l\,, \tag{3.13}$$

$$V = \sqrt{r^2 + l^2}\cos\tau/l\,, \tag{3.14}$$

the AdS_{d+1} metric on the hyperboloid (3.10) is then given by

$$g = -(1 + r^2/l^2)d\tau^2 + \frac{dr^2}{1 + r^2/l^2} + r^2 d\omega^2\,. \tag{3.15}$$

We introduce dimensionless coordinates $t = \frac{\tau}{l}$ and $x = \arctan r/l$, which transform (3.15) into

$$g = \frac{l^2}{\cos^2 x}(-dt^2 + dx^2 + \sin^2 x d\omega^2)\,, \tag{3.16}$$

where $(t, x) \in \mathbb{R} \times [0, \pi/2)$. Thus (3.15) is conformal to half of the Einstein universe $\mathbb{R} \times S^d$. Conformal infinity is given by the timelike cylinder located at the boundary $\{x = \pi/2\}$ with topology $\mathbb{R} \times S^{d-1}$. Therefore there exists no Cauchy surfaces and Anti-de Sitter is not globally hyperbolic. Given initial data one can only predict the evolution of null geodesics in the region $x < \pi$. We prove that even though the spatial distance from any point to the conformal infinity of Anti-de Sitter is infinite, null geodesics will reach it in finite coordinate time. For simplicity let us consider $d = 3$.

The Lagrangian for a geodesic motion in the metric (3.15) is then

$$\mathcal{L} = \frac{1}{2}\frac{l^2}{\cos^2 x}(-\dot{t}^2 + \dot{x}^2 + \sin^2 x(\dot{\theta}^2 + \sin^2\theta\dot{\phi}^2))\,, \tag{3.17}$$

where $\dot{} \equiv \mathrm{d}/\mathrm{d}\lambda$ denotes the differentiation with respect to the affine parameter λ. For a null geodesic we have

$$\frac{l^2}{\cos^2 x}(-dt^2 + dx^2 + \sin^2 x d\omega^2) = 0\,. \tag{3.18}$$

Because of spherical symmetry, we can fix the angles of S^2 $(\mathrm{d}\omega^2 = 0)$ and get

$$\dot{t}^2 = \dot{x}^2\,. \tag{3.19}$$

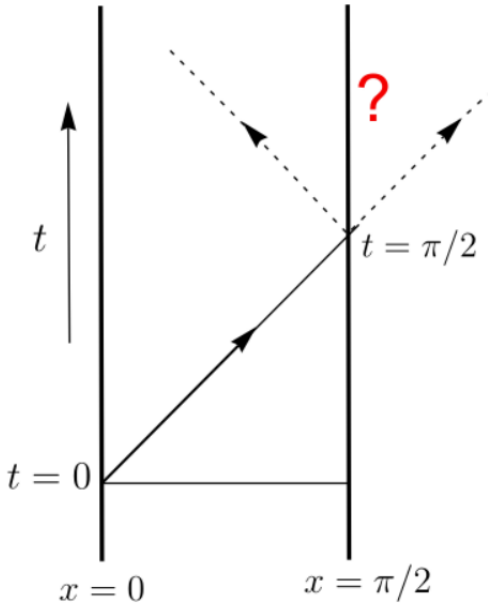

Figure 3.2.1: Conformal diagram of $d+1$ dimensional AdS space. Every point represents $\mathbb{S}^{d-1}$. A null geodesic starting from $t = 0$ and $x = 0$ will reach the conformal boundary located at $x = \pi/2$ in finite coordinate time $t = \pi/2$. From this point we can only predict the future evolution with an additional information, that is the boundary condition at the conformal boundary.

The Euler-Lagrange equation of (3.17) reads

$$\frac{d}{d\lambda}\left(\frac{l^2}{\cos^2 x}\frac{dt}{d\lambda}\right) = 0\,, \tag{3.20}$$

$$\dot{t} = \frac{E\cos^2 x}{l^2}\,. \tag{3.21}$$

Inserting (3.21) into (3.19) yields

$$\dot{x} = \pm\frac{E\cos^2 x}{l^2},, \tag{3.22}$$

$$x = \arctan\left(\pm\frac{E\lambda}{l^2}\right)\,, \tag{3.23}$$

with affine parameter λ. Therefore as $\lambda \to \infty$ $x \to \pi/2$, as AdS is geodesically complete. Then from (3.19) we conclude

$$t = \arctan\left(\pm\frac{E\lambda}{l^2}\right)\,. \tag{3.24}$$

Again from $\lambda \to \infty$ follows $t = \pi/2$, i.e. it takes finite coordinate time $t = \pi/2$ for a null geodesic to reach the boundary. After this point, the evolution depends on the boundary conditions at conformal infinity, see Fig. 3.2.1. Finally we will derive geometric properties of Anti-de Sitter. From (3.9) we find that the scalar curvature is given by

$$R = -\frac{d(d+1)}{l^2}\,. \tag{3.25}$$

As for a maximally symmetric space-times [52] we can write the curvature tensor as

$$R_{\mu\nu\rho\sigma} = \kappa\left(g_{\mu\rho}g_{\nu\sigma} - g_{\rho\nu}g_{\sigma\mu}\right)\,. \tag{3.26}$$

We can determine κ from contracting the curvature tensor and comparing with the scalar curvature (3.25), which yields $\kappa = -1/l^2$. The Ricci tensor is then given by

$$R_{\mu\nu} = -\frac{d}{l^2}g_{\mu\nu}\,, \tag{3.27}$$

3.3 Einstein static universe

We repeat basic facts and definitions of the Einstein universe based on [51] and [49]. We are looking for an idealised model of the universe, which is homogeneous and isotropic. A family of spacetimes with these properties is the Friedmann–Lemaître–Robertson–Walker metric in spherical coordinates

$$\mathrm{d}s^2 = -\mathrm{d}t^2 + R^2(t)\left(\frac{\mathrm{d}r^2}{1-kr^2} + r^2\mathrm{d}\omega^2\right) \tag{3.28}$$

with $\mathrm{d}\omega^2$ being the round metric of the unit two-sphere S^2 and $k = 0, \pm 1$ depending on the spatial curvature. The function $R(t)$ can be determined by the equations

$$3\frac{\dot{R}^2 + k}{R^2} = \Lambda + 8\pi\rho\,, \tag{3.29}$$

$$2\frac{\ddot{R}}{R} + \frac{\dot{R}^2 + k}{R^2} = \Lambda - 8\pi p\,. \tag{3.30}$$

These differential equations follow from the Einstein equation (3.9) with the energy-momentum tensor of a perfect fluid

$$T_{\mu\nu} = (\rho + p)u_\mu u_\nu + p g_{\mu\nu}\,, \tag{3.31}$$

with the energy density $\rho = \rho(t)$, the pressure $p = p(t)$ and $u^\mu\partial_\mu = \partial_t$. Equation (3.29) is often referred to as the *Friedmann equation*. For a static solution $R = R_0 = const$ the equations (3.29) and (3.30) can be satisfied by

$$R = R_0, \quad \Lambda = 4\pi\rho = \frac{1}{R_0^2}, \quad p = 0\,. \tag{3.32}$$

This characterises a solution with constant non-zero density ρ and zero pressure p, while the cosmological constant is $\Lambda > 0$. This solution is called the *Einstein universe*. The solution occurs when $k = +1$ and we can therefore write (3.28) with the coordinate transformation $r = \sin x$ as

$$\mathrm{d}s^2 = -\mathrm{d}t^2 + R_0^2\left(\mathrm{d}x^2 + \sin^2 x\mathrm{d}\omega^2\right)\,, \tag{3.33}$$

where $x \in [0, \pi]$ and $t \in (-\infty, \infty)$.By rescaling $t \to R_0 t$, (3.33) transforms to

$$\mathrm{d}s^2 = R_0^2\left(-\mathrm{d}t^2 + \mathrm{d}x^2 + \sin^2 x\mathrm{d}\omega^2\right)\,. \tag{3.34}$$

Chapter 4

Yang-Mills on Einstein universe

In this chapter, we derive the equations of motion for the Yang-Mills (YM) field propagating on the Einstein universe. We show that this problem can be reduced to a singular nonlinear PDE. By considering linear perturbations around the static solutions of this PDE, we get the eigenvalue problem for a self-adjoint operator.

4.1 The Yang-Mills field

The YM potential $A_\mu = A^a_\mu \tau_a$, where τ_a form a basis for the group $SU(2)$ with the properties $[\tau_a, \tau_b] = \epsilon^{abc}\tau_c$ and $\tau_a\tau_b = \delta_{ab}$ with $a, b, c \in \{r, \theta, \phi\}$ define the YM field strength tensor [53]

$$F^a_{\mu\nu} = \partial_\mu A^a_\nu - \partial_\nu A^a_\mu + \epsilon^{abc} A^b_\mu A^c_\nu \,, \tag{4.1}$$

The Lagrangian density is given by

$$\mathcal{L} = Tr(F^a_{\alpha\beta} F^a_{\mu\nu} g^{\alpha\mu} g^{\beta\nu})\sqrt{-g} \,, \tag{4.2}$$

where the trace is taken over the group indices. If we consider a conformally related metric $g = \Omega^2 \hat{g}$ and the YM potential $\hat{A}_\mu = A_\mu$ (4.2) yields

$$F_{\alpha\beta} F_{\mu\nu} g^{\alpha\mu} g^{\beta\nu} \sqrt{-g} = \Omega^{d-3} F_{\alpha\beta} F_{\mu\nu} \hat{g}^{\alpha\mu} \hat{g}^{\beta\nu} \sqrt{-\hat{g}} \,, \tag{4.3}$$

for a $(d+1)$ dimensional space-time. Hence for $d = 3$, solving the YM equations

$$\nabla_\mu F^{\mu\nu} + [A_\mu, F^{\mu\nu}] = 0 \,. \tag{4.4}$$

in one metric g also solves them in any conformally related metric $\hat{g}$. Therefore instead of the Anti-de Sitter space we can consider the Einstein universe and evade the inconvenience of choosing boundary conditions by extending the domain to the whole three-sphere.

The Yang-Mills equations do not develop singularities on AdS space-time, shown in [54], as well as on smooth globally hyperbolic four dimensional manifolds [55]. However, the evolution of data close to the static solution of the YM equations is still not fully explored. The long-time behaviour of these small solutions will be examined in this thesis.

4.2 Derivation of the Yang Mills equation

We study the $SU(2)$ Yang-Mills field propagating on the Einstein universe

$$ds^2 = -dt^2 + d\Omega_3^2 \,, \tag{4.5}$$

with the metric on a round sphere given by

$$d\Omega_3^2 = dx^2 + \sin^2 x (d\theta^2 + \sin^2\theta d\phi^2) \,, \tag{4.6}$$

and coordinate ranges $x, \theta \in [0, \pi]$ and $\phi \in [0, 2\pi)$.
For the Yang Mills field the most general spherically symmetric parameterisation of the gauge connection can be written as [53]

$$A = W_1\tau_3 dt + W_2\tau_3 dx + (W_3\tau_1 + W_4\tau_2)d\theta + (\cot\theta\tau_3 + W_3\tau_2 - W_4\tau_1)\sin\theta d\phi\,, \tag{4.7}$$

where the coefficients W_1, W_2, W_3, and W_4 will all depend on t and r. For our work we will make the "magnetic ansatz" from [56] and use the "abelian gauge" representation [57] by choosing $W_1, W_2, W_4 = 0$. The Yang Mills connection with $W_3 \equiv W$ then reads

$$A = W\tau_1 d\theta + (\cot\theta\tau_3 + W\tau_2)\sin\theta d\phi\,. \tag{4.8}$$

The field strength tensor (4.1) is then given by

$$\begin{aligned} F = &(\dot{W}\tau_1 dt + W'\tau_1 dx) \wedge d\theta \\ &+ (\dot{W}\tau_2 dt + W'\tau_2 dx - (1-W^2)\tau_3 d\theta) \wedge \sin\theta d\phi\,, \end{aligned} \tag{4.9}$$

where the notation $\dot{} \equiv \partial_t$ and $' \equiv \partial_x$ is used. The action function of the Yang Mills field then yields

$$S = \int Tr(F_{\mu\nu}F^{\mu\nu})\sqrt{-g}d^{d+1}x\,. \tag{4.10}$$

For the contravariant expression of F in (4.10) we calculate $F_{\mu\nu}g^{\alpha\mu}g^{\beta\nu}$, with the inverse of the metric tensor given by

$$g^{\mu\nu} = \begin{pmatrix} -1 & 0 & 0 & 0 \\ 0 & 1 & 0 & 0 \\ 0 & 0 & \csc^2 x & 0 \\ 0 & 0 & 0 & \csc^2 x \csc^2\theta \end{pmatrix}. \tag{4.11}$$

Then the contravariant Yang-Mills curvature in matrix form reads

$$F^{\mu\nu} = \begin{pmatrix} 0 & 0 & -\dot{W}\csc^2 x\,\tau_1 & -\dot{W}\csc x\csc^2\theta\,\tau_2 \\ 0 & 0 & W'\csc^2 x\,\tau_1 & W'\csc^2 x\csc\theta\,\tau_2 \\ \dot{W}\csc^2 x\,\tau_1 & -W'\csc^2 x\,\tau_1 & 0 & -(1-W^2)\csc^4 x\csc\theta\,\tau_3 \\ \dot{W}\csc x\csc^2\theta\,\tau_2 & -W'\csc^2 x\csc\theta\,\tau_2 & (1-W^2)\csc^4 x\csc\theta\,\tau_3 & 0 \end{pmatrix}. \tag{4.12}$$

The action functional reduces to

$$S = 4\pi\int\left(-\ddot{W}^2 + W'^2 + \frac{(1-W^2)^2}{2\sin^2 x}\right)dxdt\,. \tag{4.13}$$

From this, one can derive the equation of motion, using

$$\partial_\mu\frac{\partial\mathcal{L}}{\partial_\mu W} - \frac{\partial\mathcal{L}}{\partial W} = 0\,, \tag{4.14}$$

and we finally get the YM equation for the potential W

$$\partial_t^2 W = \partial_x^2 W + \frac{W(1-W^2)}{\sin^2 x}\,. \tag{4.15}$$

Alternatively the equation of motion can also be obtained from the Euler-Lagrange equation (4.4). To calculate the covariant derivative one needs to compute the Christoffel symbols $\Gamma^\lambda_{\mu\nu}$ for the metric (4.17) as

$$\begin{aligned} &\Gamma^x_{\theta\theta} = -\sin x\cos x, \quad \Gamma^x_{\phi\phi} = -\sin x\cos x\sin^2\theta\,, \\ &\Gamma^\theta_{x\theta} = \Gamma^\theta_{\theta x} = \cot x, \quad \Gamma^\theta_{\phi\phi} = -\sin\theta\cos\theta\,, \\ &\Gamma^\phi_{x\phi} = \Gamma^\phi_{\phi x} = \cot x, \quad \Gamma^\phi_{\theta\phi} = \Gamma^\phi_{\phi\theta} = \cot\theta\,, \end{aligned} \tag{4.16}$$

where all other symbols are zero. Therefore the components of the covariant derivative are

$$\nabla_\mu F^{\mu\nu} = \begin{pmatrix} \dot{W}\cot\theta\csc^2 x\ \tau_1 \\ -W'\cot\theta\csc^2 x\ \tau_1 \\ (-\ddot{W}+W'')\csc^2 x\ \tau_1 \\ (-\ddot{W}+W'')\csc^2 x\csc\theta\ \tau_2 \end{pmatrix}, \tag{4.17}$$

and

$$[A_\mu, F^{\mu\nu}] = \begin{pmatrix} -\dot{W}\cot\theta\csc^2 x\ \tau_1 \\ +W'\cot\theta\csc^2 x\ \tau_1 \\ -W(W^2-1)\csc^4 x\ \tau_1 \\ -W(W^2-1)\csc^4 x\csc\theta\ \tau_2 \end{pmatrix}. \tag{4.18}$$

Plugging (4.17) and (4.18) into (4.4) we recover the YM equation.
The conserved energy of (4.14) is then given by

$$E(W) = \frac{1}{2}\int_0^\pi \left((\partial_t W)^2 + (\partial_x W)^2 + \frac{(1-W^2)^2}{2\sin^2 x} \right), \tag{4.19}$$

which induces the regularity condition $W(t,0) = W(t,\pi) = \pm 1$. Therefore we get two distinct topological sectors. Normally we would not need to have boundary conditions because W is defined on a compact domain but we are looking for finite energy solutions. Solutions with initial data in a sector stay in that sector during time evolution. Normally we would not need to have boundary conditions because W is defined on a compact domain but we are looking for finite energy solutions

$$W(t=0,x) = f(x)\,, \tag{4.20}$$
$$\partial_t W(t=0,x) = g(x)\,. \tag{4.21}$$

Note that equation (4.14) has a reflection symmetry, which means if W is a solution then $-W$ is also a solution.

4.3 Linear perturbations

The static solution of (4.14) satisfies the differential equation

$$0 = \partial_x^2 S + \frac{S(1-S^2)}{\sin^2 x}\,. \tag{4.22}$$

In each sector exists a unique static solution. The trivial solution $S_0(x) = 1$ with energy $E = 0$ and the nontrivial solution $S_1(x) = \cos x$ found by [58] with energy $E = 3\pi/8$. Linearisation around these static solutions $S_N(x), N = 0, 1$ leads to

$$W(t,x) = S_N(x) + u(t,x)\,, \tag{4.23}$$
$$\partial_t^2 u + L(S_N)u + f(u) = 0\,, \quad u(t,x=0) = 0 = u(t,x=\pi)\,, \tag{4.24}$$

where the self-adjoint operator L on the Hilbert space $L^2([0,\pi], dx)$ is given by

$$L = -\partial_x^2 + \frac{3S_N^2 - 1}{\sin^2 x}\,, \tag{4.25}$$

and the nonlinearity by

$$f(u) = \frac{3S_N + u}{\sin^2 x}u^2\,. \tag{4.26}$$

Dropping the nonlinear part of (4.24) and separation of variables $u(t,x) = e^{i\omega_j t} e_j(x)$ yields the eigenvalue problem

$$\omega_j^2 e_j(x) = L e_j(x)\,. \tag{4.27}$$

with eigenfunctions as

$$e_j(x) = N_j \sin^2 x P_j^{(3/2,3/2)}(\cos x)\,, \tag{4.28}$$

$$N_j = \frac{\sqrt{\frac{(j+2)!(j+3)!}{2(j+2)}}}{2(j+3/2)!}\,, \tag{4.29}$$

where $P_j^{(3/2,3/2)}(z)$ are the Jacobi polynomials. The eigenmodes of L satisfy

$$(e_j|e_k) = \delta_{jk}\,, \tag{4.30}$$

with the inner product on the Hilbert space defined as

$$(f|g) := \int_0^\pi f(x)g(x)dx\,. \tag{4.31}$$

The eigenvalues are given as

$$\begin{aligned} \omega_j^2 &= \begin{cases} (j+2)^2\,, & S_0(x) \\ (j+2)^2 - 3\,, & S_1(x) \end{cases} \\ j &= 0,1,2,\ldots\,. \end{aligned} \tag{4.32}$$

The eigenvalues ω_j are natural numbers, therefore the solutions are linearly stable in both cases of $S(x)$. The eigenfunctions are the same for both static solutions due to the fact that their operators L commute. The difference in the eigenvalues has consequences for the dynamical behaviour of each solution. For S_0 we have equally spaced eigenvalues and therefore a resonant spectrum, whereas for S_1 eigenvalues are only asymptotically equidistant. It is expected that the latter case leads to limited turbulent behaviour. Evolution of data close to S_0 leads to resonant energy transfer and therefore turbulent behaviour. This energy transfer between the modes α_j can be measured by the Sobolev norms [59]. The Sobolev norms are defined as

$$||u(t,\cdot)||_s := \left(\sum_{j\geq} \omega_j^{2s} |\alpha_j|^2\right)^{\frac{1}{2}}\,. \tag{4.33}$$

As shown in [24], in the S_1 case, the Sobolev norms saturate very fast and stay bounded. Energy flow between the modes is limited which is also shown in the energy spectra, as it equilibrates very fast. Therefore we will from now on only consider the resonant case $S_0 = 1$.

Chapter 5

Derivation of resonant system

In this chapter we will derive the resonant system for the Yang-Mills equation on the Einstein universe. First we show how naïve perturbation theory produces secular terms that may accumulate on long time scales and therefore invalidate solution. In order to remove these secular terms we introduce a new time variable and hence find an approximation for the exact solution. We also find an explicit formula for the interaction coefficients of this resonant system. Lastly we show the symmetries that this resonant system possess. We begin with the weakly non-linear perturbation analysis. For small $\varepsilon \ll 1$ we expand the solution

$$u(t,x) = \varepsilon u^{(1)}(t,x) + \varepsilon^2 u^{(2)}(t,x) + \varepsilon^3 u^{(3)}(t,x) + \dots \,. \tag{5.1}$$

5.1 First order

At the leading order, we recover the linearised problem

$$\partial_t^2 u^{(1)} + L(S)u^{(1)} = 0\,, \tag{5.2}$$

thus a generic solution can be written as

$$u^{(1)}(t,x) = \sum_{j\geq 0} c_j^{(1)}(t)e_j(x) = \sum_{j\geq 0} \left(\alpha_j e^{i\omega_j t} + \bar{\alpha}_j e^{-i\omega_j t}\right) e_j(x)\,. \tag{5.3}$$

The coefficients α_j are determined by the initial conditions $u(t,x)|_{t=0}$ and $\partial_t u(t,x)|_{t=0}$.

5.2 Second order

Only looking at the second order terms we get

$$\partial_t^2 u^{(2)} + Lu^{(2)} = -\frac{3\left(u^{(1)}\right)^2}{\sin^2 x}\,, \tag{5.4}$$

and make the ansatz

$$u^{(2)}(t,x) = \sum_{l\geq 0} c_l^{(2)}(t)e_l(x)\,. \tag{5.5}$$

By projecting (5.4) onto the eigenmode $e_l(x)$ and using the property (4.30) we obtain a system of second order differential equations

$$\frac{d^2}{dt^2}c_l^{(2)}(t) + \omega_l^2 c_l^{(2)}(t) = -(s^{(2)}|e_l)\,, \quad s^{(2)} = \frac{3(u^{(1)})^2}{\sin^2 x}\,, \tag{5.6}$$

First we verify that there are no resonances present in (5.6). We therefore show that no secular terms appear in the projection

$$(s^{(2)}|e_n) = s_n^{(2)}(t) = 3\sum_{jk} c_j^{(1)}(t)c_k^{(1)}(t)\left(\frac{e_j e_k}{\sin^2 x}\middle| e_n\right) = 3\sum_{jk} c_j^{(1)}(t)c_k^{(1)}(t)M_{jkn}$$
$$= 3\sum_{jk}\left(\alpha_j\alpha_k e^{i(\omega_j+\omega_k)t} + \alpha_j\bar{\alpha}_k e^{i(\omega_j-\omega_k)t} + \bar{\alpha_j}\alpha_k e^{i(-\omega_j+\omega_k)t} + \bar{\alpha}_j\bar{\alpha}_k e^{i(-\omega_j-\omega_k)t}\right)M_{jkn}\,, \quad (5.7)$$

where we introduced

$$M_{jkn} = \left(\frac{e_j e_k}{\sin^2 x}\middle| e_n\right)\,, \quad (5.8)$$

see Sec. 5.4 for computation and properties of this integral.

By projecting the source term onto the Fourier mode $e^{-i\omega_n t}$ we are checking if the r.h.s. of (5.6) acquires a resonant term, i.e. a secular term that appears if the inhomogeneity is itself a solution of the homogeneous equation [17]. Such a secular term causes the solution to grow rapidly by at least a factor of t. By (5.7) we get

$$\int_0^{2\pi} dt\, s_n^{(2)}(t)e^{-i\omega_n t} = 3\int_0^{2\pi} dt \sum_{jk}\Big(\alpha_j\alpha_k e^{i(\omega_j+\omega_k-\omega_n)t}$$
$$+\alpha_j\bar{\alpha}_k e^{i(\omega_j-\omega_k-\omega_n)t} + \bar{\alpha_j}\alpha_k e^{i(-\omega_j+\omega_k-\omega_n)t} + \bar{\alpha}_j\bar{\alpha}_k e^{i(-\omega_j-\omega_k-\omega_n)t}\Big)M_{jkn}\,, \quad (5.9)$$

which is only non-zero for combinations of $\pm\omega_j \pm \omega_k - \omega_n = 0$. As we show in 5.4 all the terms in (5.9) are equal to zero as for $\omega_j + \omega_k = \omega_n$, $\omega_j - \omega_k = \omega_n$ and $-\omega_j + \omega_k = \omega_n$ the M_{jkn} vanish. Note that $-\omega_j - \omega_k \neq \omega_n$ is not possible for any $j, k, n \in \mathbb{N}_0$. We conclude that there are no resonant terms at the second perturbative order.

The solution of the system of differential equations (5.6) with initial conditions $c_l^{(2)}(0) = 0 = \frac{d}{dt}c_l^{(2)}(0)$ is

$$c_l^{(2)}(t) = -\frac{1}{\omega_l}\left(\sin\omega_l t\int_0^t s_n^{(2)}(\xi)\cos\omega_l\xi d\xi - \cos\omega_l t\int_0^t s_n^{(2)}(\xi)\sin\omega_l\xi d\xi\right)\,, \quad (5.10)$$

Using (5.7) we get

$$c_n^{(2)}(t) = 3\sum_{jk} M_{jkn}\left(-\frac{1}{\omega_n}\right)\left(\sin\omega_l t\int_0^t c_j^{(1)}(\xi)c_k^{(1)}(\xi)\cos\omega_l\xi d\xi\right.$$
$$\left. - \cos\omega_l t\int_0^t c_j^{(1)}(T)c_k^{(1)}(\xi)\sin\omega_l\xi d\xi\right)\,, \quad (5.11)$$

Performing the ξ integral we obtain

$$c_n^{(2)}(t) = 3\sum_{jk} M_{jkn}\left(Z_{jkn}^{++}\alpha_j\alpha_k e^{i(\omega_i+\omega_k)t} + Z_{jkn}^{--}\bar{\alpha}_j\bar{\alpha}_k e^{i(-\omega_i-\omega_k)t}\right.$$
$$+ Z_{jkn}^{+-}\alpha_j\bar{\alpha}_k e^{i(\omega_i-\omega_k)t} + Z_{jkn}^{-+}\bar{\alpha}_j\alpha_k e^{i(-\omega_i+\omega_k)t}$$
$$\left. + Z_{jkn}(\alpha)e^{i\omega_n t} + \bar{Z}_{jkn}(\alpha)e^{-i\omega_n t}\right)\,, \quad (5.12)$$

where

$$Z_{jkn}^{++} = \frac{1}{(\omega_j+\omega_k)^2 - \omega_n^2} = Z_{jkn}^{--}\,, \quad (5.13)$$

$$Z_{jkn}^{+-} = \frac{1}{(\omega_j-\omega_k)^2 - \omega_n^2} = Z_{jkn}^{-+}\,, \quad (5.14)$$

$$Z_{jkn}(\alpha) = -\frac{1}{2\omega_n}\left(\frac{\alpha_j\alpha_k}{\omega_j+\omega_k-\omega_n} + \frac{\bar{\alpha}_j\alpha_k}{-\omega_j+\omega_k-\omega_n}\right. \quad (5.15)$$

$$\left. + \frac{\alpha_j\bar{\alpha}_k}{\omega_j-\omega_k-\omega_n} + \frac{\bar{\alpha}_j\bar{\alpha}_k}{-\omega_j-\omega_k-\omega_n}\right)\,, \quad (5.16)$$

5.3 Third order

The differential equation at the third order is given by

$$\partial_t^2 u^{(3)} + L u^{(3)} = -\frac{6u^{(1)}u^{(2)} + (u^{(1)})^3}{\sin^2 x}\,, \tag{5.17}$$

As before we make an ansatz

$$u^{(3)}(t,x) = \sum_{j\geq 0} c_j^{(3)}(t) e_j(x)\,. \tag{5.18}$$

Using (5.18) and projecting (5.17) onto the mode $e_l(x)$ we get a system of coupled differential equations for the mode coefficients $c_l^{(3)}$

$$\begin{aligned}\frac{d^2}{dt^2}c_n^{(3)}(t) + \omega_n^2 c_n^{(3)}(t) &= \Big(s^{(3)}\Big|\, e_n\Big) \\ &= -6\sum_{jk} c_j^{(1)}c_k^{(2)}\Big(\frac{e_j e_k}{\sin^2 x}\Big|\, e_n\Big) - \sum_{jkl} c_j^{(1)}c_k^{(1)}c_l^{(1)}\Big(\frac{e_j e_k e_l}{\sin^2 x}\Big|\, e_n\Big)\,,\end{aligned} \tag{5.19}$$

which using (5.8) and

$$K_{jkln} = \left(\frac{e_j e_k e_l}{\sin^2 x}\Big|\, e_n\right)\,, \tag{5.20}$$

can be written as

$$\frac{d^2}{dt^2}c_n^{(3)}(t) + \omega_n^2 c_n^{(3)}(t) = -6\sum_{jk} c_j^{(1)}c_k^{(2)} M_{jkn} - \sum_{jkl} c_j^{(1)}c_k^{(1)}c_l^{(1)} K_{jkln}\,, \tag{5.21}$$

For the computation and properties of K_{jkln} see Sec. 5.4. Next, as in the second perturbative order we look for resonant terms in the source $s^{(3)}$. Thus, as before we project onto the Fourier mode,

$$\int_0^{2\pi} dt\,\Big(s^{(3)}\Big|\, e_n\Big)\, e^{-i\omega_n t}\,. \tag{5.22}$$

For the cubic part of (5.22) we find

$$\begin{aligned}\int_0^{2\pi} dt \left(\frac{\big(u^{(1)}\big)^3}{\sin^2 x}\Big|\, e_n\right) e^{-i\omega_n t} &= \sum_{jkl} K_{jkln}\int_0^{2\pi} dt c_j^{(1)}c_k^{(1)}c_l^{(1)} e^{-i\omega_n t} \\ &= \int_0^{2\pi} dt \sum_{jkl}^{\infty}\Big(\alpha_j\alpha_k\alpha_l e^{i(\omega_j+\omega_k+\omega_l-\omega_n)t}K_{jkln} + \alpha_j\bar\alpha_k\alpha_l e^{i(\omega_j-\omega_k+\omega_l-\omega_n)t}K_{jkln} \\ &+ \bar\alpha_j\alpha_k\alpha_l e^{i(-\omega_j+\omega_k+\omega_l-\omega_n)t}K_{jkln} + \bar\alpha_j\bar\alpha_k\alpha_l e^{i(-\omega_j-\omega_k+\omega_l-\omega_n)t}K_{jkln} \\ &+ \alpha_j\alpha_k\bar\alpha_l e^{i(\omega_j+\omega_k-\omega_l-\omega_n)t}K_{jkln} + \alpha_j\bar\alpha_k\bar\alpha_l e^{i(\omega_j-\omega_k-\omega_l-\omega_n)t}K_{jkln} \\ &+ \bar\alpha_j\alpha_k\bar\alpha_l e^{i(-\omega_j+\omega_k-\omega_l-\omega_n)t}K_{jkln} + \bar\alpha_j\bar\alpha_k\bar\alpha_l e^{i(-\omega_j-\omega_k-\omega_l-\omega_n)t}K_{jkln}\Big) \\ &= 2\pi\left(\sum_{jkl}^{+++}\alpha_j\alpha_k\alpha_l K_{jkln} + 3\sum_{jkl}^{++-}\alpha_j\alpha_k\bar\alpha_l K_{jkln} + 3\sum_{jkl}^{+--}\alpha_j\bar\alpha_k\bar\alpha_l K_{jkln}\right)\,,\end{aligned} \tag{5.23}$$

where we used the following notation for resonant sums:

$$\sum_{jkl}^{+++} = \sum_{\substack{j,k,l=0\\ n+2=j+2+k+2+l+2}}^{\infty}\,,\quad \sum_{jkl}^{++-} = \sum_{\substack{j,k,l=0\\ n+2=j+2+k+2-(l+2)}}^{\infty}\,,\quad \sum_{jkl}^{+--} = \sum_{\substack{j,k,l=0\\ n+2=j+2-(k+2)-(l+2)}}^{\infty}\,, \tag{5.24}$$

and the symmetry properties of K_{jkln}. Similarly as for the second perturbative order, secular terms appear whenever a combination of eigenfrequencies satisfies $\omega_j \pm \omega_k \pm \omega_l = \omega_n$. Note that $-\omega_j - \omega_k - \omega_l = -\omega_n$ is not possible for $j, k, l, n \in \mathbb{N}_0$. Using the following property

$$K_{jkln} = 0\,, \quad j + k + l + 2 < n\,, \tag{5.25}$$

which is valid for all perturbations of indices, (5.23) simplifies to

$$\int_0^{2\pi} dt \left(\frac{\left(u^{(1)}\right)^3}{\sin^2 x} \middle| e_n \right) e^{-i\omega_n t} = 2\pi \sum_{jkl}^{++-} 3K_{jkln}\alpha_j\alpha_k\bar{\alpha}_l\,. \tag{5.26}$$

Therefore, the only resonant contribution coming from $(u_1)^3$ term is the $\omega_j + \omega_k - \omega_l = \omega_n$ combination, denoted as the $++-$ sum in (5.26).

For the $u^{(1)}u^{(2)}$ term we find

$$\begin{aligned}
&\int_0^{2\pi} dt \left(\frac{6u^{(1)}u^{(2)}}{\sin^2 x} \middle| e_n \right) e^{-i\omega_n t} = 6\int_0^{2\pi} dt \sum_{jk} c_j^{(1)} c_k^{(2)} \left(\frac{e_j e_k}{\sin^2 x} \middle| e_n \right) e^{-i\omega_n t} \\
&= 6\int_0^{2\pi} dt \sum_{jk} \left(\alpha_j e^{i\omega_j t} + \bar{\alpha}_j e^{-i\omega_j t}\right) \Bigg[3\sum_{lmk} M_{lmk} \Big(Z_{lmk}^{++}\alpha_l\alpha_m e^{i(\omega_l+\omega_m)t} + Z_{lmk}^{--}\bar{\alpha}_l\bar{\alpha}_m e^{i(-\omega_l-\omega_m)t} \\
&\qquad + Z_{lmk}^{+-}\alpha_l\bar{\alpha}_m e^{i(\omega_l-\omega_m)t} + Z_{lmk}^{-+}\bar{\alpha}_l\alpha_m e^{i(\omega_l-\omega_m)t} \\
&\qquad + Z_{lmk}(\alpha)e^{i\omega_k t} + \bar{Z}_{lmk}(\alpha)e^{-i\omega_k t} \Big) \Bigg] M_{jkn} e^{-i\omega_n t}\,.
\end{aligned} \tag{5.27}$$

Using the property

$$M_{jkn} = 0\,, n > j + k\,, \tag{5.28}$$

if any of the indices is bigger we can show that

1. for Z_{lmk}^{++} term with the $e^{i\omega_j t}$ factor:

$$\begin{aligned}
\omega_l + \omega_m + \omega_j = \omega_n &\Rightarrow l + m = -j + n - 4\,, \\
k > l + m &\Rightarrow k > n - j - 4 \Rightarrow M_{lmk} = 0\,, \\
n > j + k &\Rightarrow k < n - j \Rightarrow M_{jkn} = 0\,,
\end{aligned}$$

   which means for every $k \in \mathbb{N}$, k is always either bigger than $n-j-4$ or smaller than $n-j$ for all possible n, j and therefore M_{jkn} or M_{lmk} is zero, so the whole term vanishes.

2. for Z_{lmk}^{++} term with the $e^{-i\omega_j t}$ factor:

$$\begin{aligned}
\omega_l + \omega_m - \omega_j = \omega_n &\Rightarrow l + m = j + n\,, \\
k > l + m &\Rightarrow k > j + n \Rightarrow M_{abj} = 0\,, \\
n > k + j &\Rightarrow k < n - jM_{ijl} = 0\,,
\end{aligned}$$

   which means there exist $k \in \mathbb{N}$ for which these integrals do not vanish.

3. for $Z_{lmk}(\alpha)$ with the $e^{-i\omega_j t}$ factor:

$$\begin{aligned}
-\omega_j + \omega_k = \omega_n &\Rightarrow j = k - n - 2\,, \\
k > n + j &\Rightarrow k > k - 2 \Rightarrow M_{jkn} = 0\,,
\end{aligned}$$

   so for all $k \in \mathbb{N}, M_{jkn}$ is always zero.

Going through every term in a similar fashion, we find that (5.26) reduces to

$$\begin{aligned}\int_0^{2\pi} dt \left(\frac{6u^{(1)}u^{(2)}}{\sin^2 x}|e_n\right) e^{-i\omega_n t} &= \int_0^{2\pi} dt 18 \sum_{jk}\sum_{ml} \Big(Z^{+-}_{lmk}\alpha_j\alpha_l\bar{\alpha}_m e^{i(\omega_j+\omega_l-\omega_m-\omega_n)t} \\ &\quad + Z^{-+}_{lmk}\alpha_j\bar{\alpha}_l\alpha_m e^{i(\omega_j-\omega_l+\omega_m-\omega_n)t} + Z^{++}_{lmk}\bar{\alpha}_j\alpha_l\alpha_m e^{i(-\omega_j+\omega_l+\omega_m-\omega_n)t}\Big) M_{lmk}M_{jkn} \\ &= 2\pi 18 \sum_k \left(\sum_{jlm}^{++-} \alpha_j\alpha_l\bar{\alpha}_m (Z^{+-}_{lmk}M_{lmk} + Z^{-+}_{mlk}M_{mlk})M_{jkn} + \sum_{ljm}^{++-} \alpha_j\alpha_l\bar{\alpha}_m Z^{++}_{ljk}M_{ljk}M_{mkn}\right), \end{aligned} \tag{5.29}$$

where in the last equality we renamed the indices appropriately. Next, using $Z^{++}_{ljk} = Z^{++}_{jlk}$ and the following symmetries $Z^{+-}_{lmk} = Z^{-+}_{mlk}$ and $M_{ljk} = M_{jlk}$, see (5.13) and (5.15) respectively, we get

$$\begin{aligned}\int_0^{2\pi} dt \left(\frac{6u^{(1)}u^{(2)}}{\sin^2 x}|e_n\right) e^{-i\omega_n t} &\\ = 2\pi 18 \sum_k \left(\sum_{jlm}^{++-} \alpha_j\alpha_l\bar{\alpha}_m (2Z^{+-}_{lmk}M_{lmk}M_{jkn} + Z^{++}_{ljk}M_{ljk}M_{mkn})\right) &\\ = 2\pi 18 \sum_{jlm}^{++-} \alpha_j\alpha_l\bar{\alpha}_m \widetilde{M}_{jlmn}\,, &\end{aligned} \tag{5.30}$$

with

$$\widetilde{M}_{jlmn} = \sum_k (2Z^{+-}_{lmk}M_{lmk}M_{jkn} + Z^{++}_{ljk}M_{ljk}M_{mkn})\,, \tag{5.31}$$

Finally, the resonant terms on the RHS of (5.19) are

$$\int_0^{2\pi} dt \left(s^{(3)}|e_n\right) e^{-i\omega_n t} = -2\pi 18 \sum_{jlm}^{++-} \alpha_j\alpha_l\bar{\alpha}_m\widetilde{M}_{jlmn} - 2\pi \sum_{jkl}^{++-} 3K_{jkln}\alpha_j\alpha_k\bar{\alpha}_l\,, \tag{5.32}$$

Such terms lead to secular growth of the solution $u^{(3)}$, which invalidates perturbative expansion (5.1) at $t \sim \varepsilon^{-2}$.

5.4 Interaction Coefficients

In this section we will show some of the properties of the integrals K_{ijkl} and M_{ijk}, which we have already used in 5.2 and 5.3 to simplify the resonant terms. Using properties of the Jacobi polynomials we also derive an explicit formula for these integrals, saving us a lot of time and computational power.

5.4.1 Properties

One can easily see that the integrals

$$K_{ijkl} = \left(\frac{e_ie_je_k}{\sin^2 x}\middle| e_l\right)\,, \tag{5.33}$$

$$M_{ijk} = \left(\frac{e_ie_j}{\sin^2 x}\middle| e_k\right)\,, \tag{5.34}$$

are symmetric for all permutations of indices $i, j, k, l \in \mathbb{N}$. Another property is that these integrals will vanish for a certain set of indices. To show this, we will express the eigenfunctions in terms of Jacobi polynomials, using the coordinate transformation $y = \cos x$ [60]

$$e_n(y) \sim (1-y^2)P_n^{(3/2,3/2)}(y)\,, \tag{5.35}$$

where we skip the irrelevant numerical factors. Therefore the integral reads

$$K_{ijkl} \sim \int_{-1}^{1} dy\,(1-y^2)^{5/2} P_i^{(3/2,3/2)}(y) P_j^{(3/2,3/2)}(y) P_k^{(3/2,3/2)}(y) P_l^{(3/2,3/2)}(y)\,. \tag{5.36}$$

The Jacobi polynomial can also be expressed as [61]

$$P_n^{(\alpha,\beta)}(y) \sim (1-y)^{-\alpha}(1+y)^{-\beta}\frac{d^n}{dy^n}((1-y)^{\alpha+n}(1+y)^{\beta+n})\,, \tag{5.37}$$

which gives us

$$K_{ijkl} \sim \int_{-1}^{1} dy\,(1-y^2) P_i^{(3/2,3/2)}(y) P_j^{(3/2,3/2)}(y) P_k^{(3/2,3/2)}(y) \frac{d^l}{dy^l}((1-y)^{3/2+l}(1+y)^{3/2+l})\,. \tag{5.38}$$

Integrating by parts we find that $K_{ijkl} = 0$ if

$$l > i+j+k+2\,, \tag{5.39}$$

because $(1-y^2)P_i^{(3/2,3/2)}(y)P_j^{(3/2,3/2)}(y)P_k^{(3/2,3/2)}(y)$ is a polynomial of order $i+j+k+2$. We partially integrate (5.38) l times yields

$$K_{ijkl} \sim \int_{-1}^{1} dy\,\frac{d^l}{dy^l}\left((1-y^2) P_i^{(3/2,3/2)}(y) P_j^{(3/2,3/2)}(y) P_k^{(3/2,3/2)}(y)\right)((1-y)^{3/2+l}(1+y)^{3/2+l})\,. \tag{5.40}$$

Therefore differentiating more than $i+j+k+2$ times gives 0. Because of the symmetry of K_{ijkl} this is true for any permutation.

Analogously for the M_{ijk} integral we can write

$$M_{ijk} \sim \int_{-1}^{1} dy\, P_i^{(3/2,3/2)}(y) P_j^{(3/2,3/2)}(y) \frac{d^k}{dy^k}((1-y)^{3/2+k}(1+y)^{3/2+k})\,. \tag{5.41}$$

And with the same argumentation as before, $M_{ijk} = 0$ if

$$k > i+j\,. \tag{5.42}$$

5.4.2 Computation of the integrals

For the computation of the K_{ijkl} integral we will again use the coordinate transformation $y = \cos x$

$$\begin{aligned} K_{ijkl} &\sim \int_{-1}^{1} dy\,(1-y^2)^{3/2}(1-y^2) P_i^{(3/2,3/2)}(y) P_j^{(3/2,3/2)}(y) P_k^{(3/2,3/2)}(y) P_l^{(3/2,3/2)}(y) \\ &= \int_{-1}^{1} dy\,(1-y^2)^{3/2} P_i^{(3/2,3/2)}(y) P_j^{(3/2,3/2)}(y) P_k^{(3/2,3/2)}(y) P_l^{(3/2,3/2)}(y) \\ &\quad - \int_{-1}^{1} dy\, y^2 (1-y^2)^{3/2} P_i^{(3/2,3/2)}(y) P_j^{(3/2,3/2)}(y) P_k^{(3/2,3/2)}(y) P_l^{(3/2,3/2)}(y) \end{aligned} \tag{5.43}$$

From [62] we have the property

$$\begin{aligned} P_i^{\lambda,\lambda}(x) P_j^{\lambda,\lambda}(x) = \frac{(\lambda+1)_i(\lambda+1)_j}{(2\lambda+1)_i(2\lambda+1)_j} &\sum_{k=0}^{\min(i,j)} \frac{(\lambda+i+j-2k+\frac{1}{2})(i+j-2k)!}{(\lambda+i+j-k+\frac{1}{2})k!(i-k)!(j-k)!} \\ &\times \frac{(2\lambda+1)_{i+j-k}(\lambda+\frac{1}{2})_k(\lambda+\frac{1}{2})_{i-k}(\lambda+\frac{1}{2})_{j-k}}{(\lambda+\frac{1}{2})_{i+j-k}(\lambda+\frac{1}{2})_{ij+-2k}} P_{i+j-2k}^{(\lambda,\lambda)}(x) \\ &= \sum_{k=0}^{\min(i,j)} L_{ij}(k) P_{i+j-2k}^{(\lambda,\lambda)}(x)\,, \end{aligned} \tag{5.44}$$

which yields for the first term

$$K_{ijkl} \sim \int_{-1}^{1} dy\,(1-y^2)^{3/2} \sum_{m=0}^{\min(i,j)} \sum_{n=0}^{\min(k,l)} L_{ij}(m) L_{kl}(n) P_{i+j-2m}^{(3/2,3/2)}(y) P_{k+l-2n}^{(3/2,3/2)}(y)$$
$$= \sum_{m=0}^{\min(i,j)} \sum_{n=0}^{\min(k,l)} L_{ij}(m) L_{kl}(n) \frac{\delta_{i+j-2m,k+l-2n}}{N_{i+j-2m} N_{k+l-2n}}\,, \quad (5.45)$$

where we used the orthogonality property (4.30)

$$\int_{-1}^{1} dy\,(1-y^2)^{3/2} N_i N_j (1-y^2) P_i^{(3/2,3/2)}(y) P_j^{(3/2,3/2)}(y) = \delta_{ij}\,, \quad (5.46)$$

in the last line of (5.45). For the y^2 term of (5.43) we use the property from [63]

$$x P_n^{(a,b)}(x) = \frac{2(n+1)(n+a+b+1)}{(1+a+b+2n)(2+a+b+2n)} P_{n+1}^{(a,b)}(x)$$
$$+ \frac{b^2-a^2}{(a+b+2n)(2+a+b+2n)} P_n^{(a,b)}(x) + \frac{2(n+a)(n+b)}{(a+b+2n)(1+a+b+2n)} P_{n-1}^{(a,b)}(x)\,, \quad (5.47)$$

which is true for all $n \in \mathbb{N}_0$. Analogously we can compute the M_{ijk} integral

$$M_{ijk} \sim \int_{-1}^{1} dy\,(1-y^2)^{3/2} P_i^{(3/2,3/2)}(y) P_j^{(3/2,3/2)}(y) P_k^{(3/2,3/2)}(y)$$
$$= \int_{-1}^{1} dy\,(1-y^2)^{3/2} \sum_{m=0}^{\min(i,j)} L_{ij}(m) P_{i+j-2m}^{(3/2,3/2)}(y) P_k^{(3/2,3/2)}(y)$$
$$= \sum_{m=0}^{\min(i,j)} L_{ij}(m) \frac{\delta_{i+j-2m,k}}{N_{i+j-2m} N_k}\,. \quad (5.48)$$

With these formulas we can efficiently compute the integrals (5.32).

5.5 Resonant approximation

In order to remove the resonances from (5.32) we use the multi-scale approach [64] and repeat our perturbation analysis. Therefore we introduce the 'slow time' dependence $\tau = \epsilon^2 t$ and get

$$u = u(t, \tau, x)\,. \quad (5.49)$$

By treating the two time scales t an τ as independent variables the partial time derivative transforms to

$$\partial_t^2 u(t,x) \to \partial_t^2 u(t,\tau,x) + 2\epsilon^2 \partial_t \partial_\tau u(t,\tau,x) + \epsilon^4 \partial_\tau^2 u(t,\tau,x)\,. \quad (5.50)$$

For the solution at first order the coefficients $c_j^{(1)}(t)$ are now depending on τ, i.e. (5.3) becomes

$$u^{(1)}(t,\tau,x) = \sum_{j\geq 0} c_j^{(1)}(t,\tau) e_j(x) = \sum_{j\geq 0} \left(\alpha_j(\tau) e^{i\omega_j t} + \bar{\alpha}_j(\tau) e^{-i\omega_j t}\right) e_j(x)\,, \quad (5.51)$$

There are no changes to the second order solution (5.12), whereas at third order we get

$$\partial_t^2 u^{(3)} + 2\partial_t \partial_\tau u_n^{(1)} + L u^{(3)} = -\frac{6u^{(1)}u^{(2)} + (u^{(1)})^3}{\sin^2 x}\,, \quad (5.52)$$

c.f. (5.17). By setting the projection onto the Fourier mode $\{e^{i\omega_l t}\}$ to zero we remove the resonant terms

$$\int_0^{2\pi} dt \left(-2\partial_t\partial_\tau u^{(1)} + s^{(3)}|e_n\right) e^{-i\omega_n t} = 0\,. \tag{5.53}$$

Evaluating the integral (5.53) we get

$$\begin{aligned}\int_0^{2\pi} dt \left(-2\partial_t\partial_\tau u^{(1)} + s^{(3)}|e_n\right) e^{-i\omega_n t} = \\ \int_0^{2\pi} dt(-2)i\omega_n \left(\alpha_n'(\tau)e^{i\omega_n t} - \bar\alpha_n'(\tau)e^{-i\omega_n t}\right) e^{-i\omega_n t} + \int_0^{2\pi} dt \left(s^{(3)}|e_n\right) e^{-i\omega_n t} \\ = -4\pi i\omega_n\alpha_n'(\tau) - 2\pi 18 \sum_{jlm}^{++-} \alpha_j\alpha_l\bar\alpha_m\widetilde{M}_{jlmn} - 2\pi \sum_{jkl}^{++-} 3K_{jkln}\alpha_j\alpha_k\bar\alpha_l\,, \end{aligned} \tag{5.54}$$

By setting (5.53) to zero we ensure that the the solution $u^{(3)}$ is bounded. This only hold if the coefficients $\alpha_n(\tau)$ satisfy the following system of equations and therefore cancel out the resonant terms in (5.52)

$$2i\omega_n\frac{d\alpha_n}{d\tau} = -18\sum_{jlm}^{++-} \alpha_j\alpha_l\bar\alpha_m\widetilde{M}_{jlmn} - \sum_{jlm}^{++-} 3K_{jlmn}\alpha_j\alpha_l\bar\alpha_m\,, \tag{5.55}$$

where we renamed the indices in the last term. We will refer to (5.55) as the resonant system. Defining

$$S_{jlmn} = -18\widetilde{M}_{jlmn} - 3K_{jlmn}\,, \tag{5.56}$$

we rewrite (5.55) as

$$2i\omega_n\frac{d\alpha_n}{d\tau} = \sum_{jlm}^{++-} S_{jlmn}\alpha_j\alpha_l\bar\alpha_m\,. \tag{5.57}$$

Note that (5.57) is invariant under scaling

$$\alpha_n(\tau) \to \varepsilon^{-1}\alpha_n(\tau/\varepsilon^2)\,. \tag{5.58}$$

5.6 Symmetries of the resonant system

Similar to [22] the system (5.57) enjoys the following symmetries $\theta, \tau_0 \in \mathbb{R}$

$$\text{Global phase shift:} \quad \alpha_n(\tau) \to e^{i\theta}\alpha_n(\tau)\,, \tag{5.59}$$

$$\text{Mode-dependent phase shift:} \quad \alpha_n(\tau) \to e^{in\theta}\alpha_n(\tau)\,, \tag{5.60}$$

$$\text{Time translation:} \quad \alpha_n \to \alpha_n(\tau+\tau_0)\,. \tag{5.61}$$

The resonant system (5.57) is Hamiltonian with

$$H = \sum_{\substack{jlmn \\ j+l=m+n}} S_{jlmn}\alpha_j\alpha_l\bar\alpha_m\bar\alpha_n\,, \tag{5.62}$$

and the symplectic form $\sum_n 4i\omega_n d\bar\alpha_n \wedge d\alpha_n$:

$$2i\omega_n\dot\alpha_n = \frac{1}{2}\frac{\partial H}{\partial\bar\alpha}\,. \tag{5.63}$$

Chapter 6

Conserved quantities

In this section we give three conserved quantities of the resonant system (5.57) and show their conservation analytically and numerically. The symmetries (5.59)-(5.61) lead to the following three conserved quantities [65]

$$J = \sum_n \omega_n |\alpha_n|^2 \,, \tag{6.1}$$

$$E = \sum_n \omega_n^2 |\alpha_n|^2 \,, \tag{6.2}$$

$$H = \sum_{\substack{jlmn \\ j+l=m+n}} S_{jlmn} \alpha_j \alpha_l \bar{\alpha}_m \bar{\alpha}_n \,. \tag{6.3}$$

The simultaneous conservation of E and J implies that energy cannot all be transferred to higher-n modes without also transferring energy to lower-n modes, leading to more complex turbulent behaviour [66].

6.1 Conservation of E

In the following we show that $E = \sum_i \omega_i |\alpha_i|^2$ is constant along the flow generated by the resonant system. Inserting (5.57) into the derivative of E we find

$$\begin{aligned} \frac{d}{d\tau} E = \sum_l \omega_l^2 (\dot{\alpha}_l \bar{\alpha}_l + \alpha_l \dot{\bar{\alpha}}_l) &= \frac{1}{2i} \sum_l \omega_l \sum_{ijk}^{++-} (S_{ijkl} \alpha_i \alpha_j \bar{\alpha}_k \bar{\alpha}_l - S_{ijkl} \alpha_k \alpha_l \bar{\alpha}_i \bar{\alpha}_j) \\ &= \frac{1}{4i} \sum_l \sum_{ijk}^{++-} (S_{ijkl} \omega_l + S_{ijlk} \omega_k)(\alpha_i \alpha_j \bar{\alpha}_k \bar{\alpha}_l - \alpha_k \alpha_l \bar{\alpha}_i \bar{\alpha}_j) \,. \end{aligned} \tag{6.4}$$

Here we used the symmetry of the α term with respect to k and l. Next, using the identity

$$S_{ijkl} = S_{jilk} \iff i + j - k = l \,, \tag{6.5}$$

we rewrite the sum as

$$\begin{aligned} \frac{d}{d\tau} E &= \frac{1}{4i} \sum_l \sum_{ijk}^{++-} (S_{ijkl} \omega_l + S_{jikl} \omega_k)(\alpha_i \alpha_j \bar{\alpha}_k \bar{\alpha}_l - \alpha_k \alpha_l \bar{\alpha}_i \bar{\alpha}_j) \\ &= \frac{1}{2i} \sum_l \sum_{ijk}^{++-} S_{ijkl} (\omega_l + \omega_k)(\alpha_i \alpha_j \bar{\alpha}_k \bar{\alpha}_l - \alpha_k \alpha_l \bar{\alpha}_i \bar{\alpha}_j) \,, \end{aligned} \tag{6.6}$$

where we used that the α term is symmetric with respect to $(i \leftrightarrow j)$. Now we note that S_{ijkl} is symmetric under the pair exchange $(i \leftrightarrow k)$ and $(j \leftrightarrow l)$,

$$S_{ijkl} = S_{klij} \iff i + j - k = l \,, \tag{6.7}$$

therefore the contraction of $S_{ijkl}(\omega_l + \omega_k)$ with the antisymmetric α-term is zero and we get

$$\frac{d}{d\tau}E = 0\,. \tag{6.8}$$

The numerical results for two-mode initial data also indicate conservation of E, see Fig. 6.3.1.

6.2 Conservation of J

Next we show that $J = \sum_i \omega_i |\alpha_i|^2$ is conserved, see Fig. 6.3.2

$$\begin{aligned}\frac{d}{d\tau}J &= \sum_l \omega_l(\dot{\alpha}_l\bar{\alpha}_l + \alpha_l\dot{\bar{\alpha}}_l) \\ &= \frac{1}{2i}\sum_l \sum_{ijk}^{++-} S_{ijkl}(\alpha_i\alpha_j\bar{\alpha}_k\bar{\alpha}_l - \alpha_k\alpha_l\bar{\alpha}_i\bar{\alpha}_j).\end{aligned} \tag{6.9}$$

Again because of the symmetry of S_{ijkl} under the pair interchange $(i,j) \leftrightarrow (k,l)$ from (6.7) the contraction with the α term is zero, and we conclude

$$\frac{d}{d\tau}J = 0\,. \tag{6.10}$$

6.3 Conservation of H

Finally we will look at the conserved quantity $H = \sum_{ijkl} S_{ijkl}\alpha_i\alpha_j\bar{\alpha}_k\bar{\alpha}_l$. First we calculate

$$\begin{aligned}\frac{\partial H}{\partial\bar{\alpha}_n} &= \sum_{ijkl} S_{ijkl}\alpha_i\alpha_j\frac{\partial\bar{\alpha}_k}{\partial\bar{\alpha}_n}\bar{\alpha}_l + S_{ijkl}\alpha_i\alpha_j\bar{\alpha}_k\frac{\partial\bar{\alpha}_l}{\partial\bar{\alpha}_n} \\ &= \sum_{ijk} S_{jinl}\alpha_i\alpha_j\bar{\alpha}_k + S_{ijln}\alpha_i\alpha_j\bar{\alpha}_k \\ &= 2\sum_{ijk} S_{jikn}\alpha_i\alpha_j\bar{\alpha}_k \\ &= 4i\omega_n\dot{\alpha}_n\,,\end{aligned} \tag{6.11}$$

where we used the symmetry of the α term with respect to $(i \leftrightarrow j)$ and (6.5). The derivative $\frac{\partial H}{\partial\alpha_n}$ can be calculated analogously

$$\frac{\partial H}{\partial\alpha}_n = -4i\omega_n\dot{\bar{\alpha}}_n\,. \tag{6.12}$$

Hence we get

$$\begin{aligned}\frac{d}{d\tau}H &= \sum_n \left(\frac{\partial H}{\partial\alpha_n}\dot{\alpha}_n + \frac{\partial H}{\partial\bar{\alpha}_n}\dot{\bar{\alpha}}_n\right) \\ &= \sum_n \left(4i\omega_n\dot{\bar{\alpha}}_n\dot{\alpha}_n - 4i\omega_n\dot{\alpha}_n\dot{\bar{\alpha}}_n\right) = 0\,,\end{aligned} \tag{6.13}$$

and therefore H is conserved. The numerical evolution of H for two mode initial data is shown in 6.3.3.

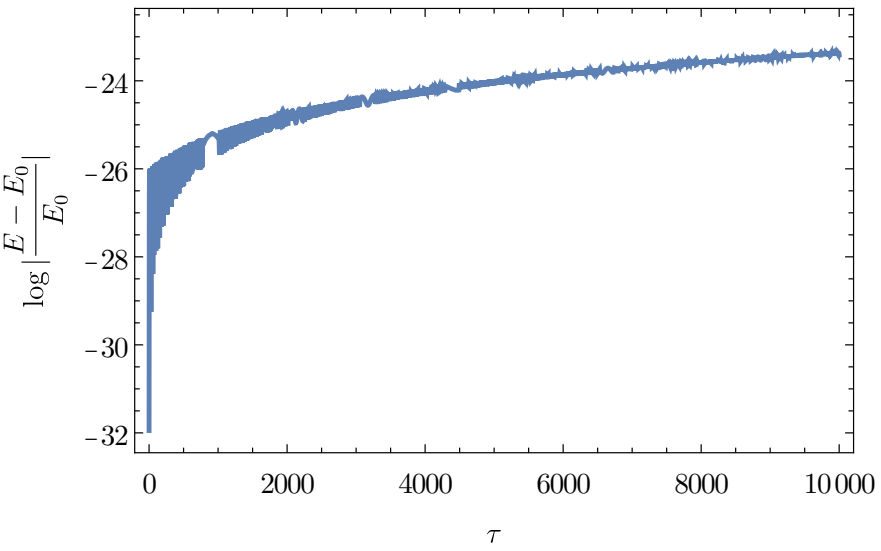

Figure 6.3.1: Evolution of the absolute value of the relative error $\frac{E-E_0}{E_0}$ of the quantity E with two-mode initial data truncated to 64 modes. We conclude that E is conserved.

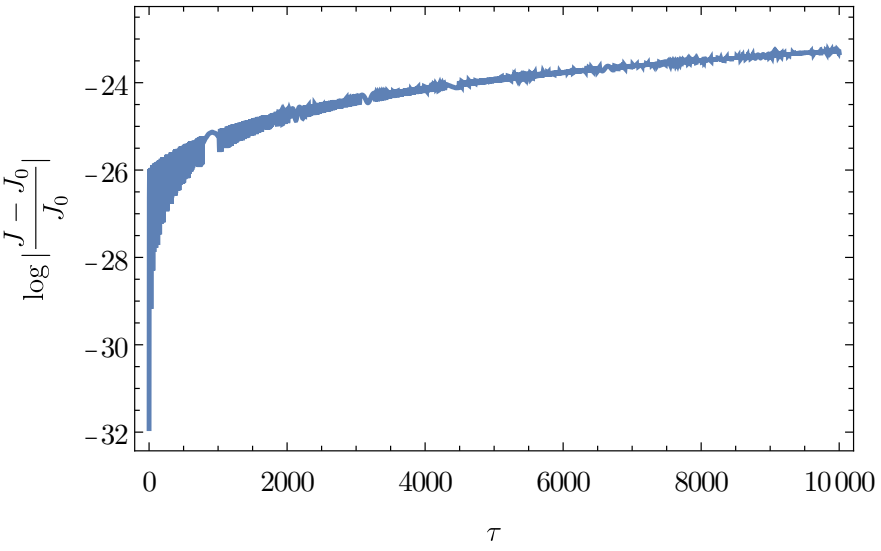

Figure 6.3.2: Evolution of the absolute value of the relative error $\frac{J-J_0}{J_0}$ of the quantity J with two-mode initial data truncated to 64 modes. We conclude that J is conserved.

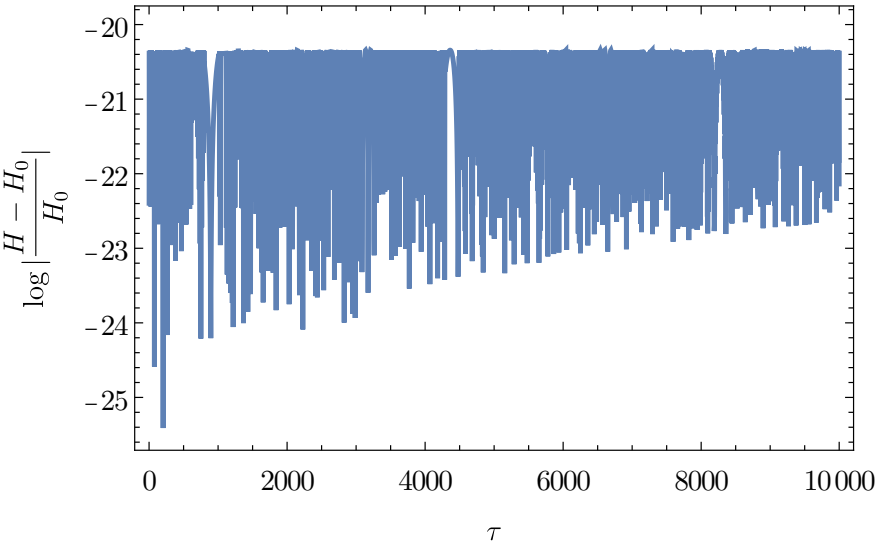

Figure 6.3.3: Evolution of the absolute value of the relative error $\frac{H-H_0}{H_0}$ of the quantity H with two-mode initial data truncated to 64 modes. We conclude that H is conserved.

Chapter 7

Comparison to PDE solution

In this Chapter we compare our resonant system to the PDE-solution and show that the resonant system indeed gives a good approximation for timescales $\mathcal{O}(\varepsilon^{-2})$. We will be comparing the coefficients of both solutions via the ansatz (5.51).

7.1 Numerical solution of the PDE

For the PDE solution we consider the nonlinear partial differential equation (4.24)

$$\partial_t^2 u = -Lu - \frac{3+u}{\sin^2 x} u^2 \,. \tag{7.1}$$

We evaluate the PDE on the grid

$$x_i = \frac{2i-1}{2N}\pi \,, \quad i = 1, ..., N \,. \tag{7.2}$$

Generally in the Spectral approach [67], one chooses the zeros of eigenfunctions as the grid. In our case the zeros of (4.28) are non-equidistant, hence we use the grid (7.2), which is equidistant and the best analytic approximation for the zeros of the eigenfunctions [68]. We can then write the operator (4.25) as

$$(Lu)_i = -(\partial_x^2 u)_i + \frac{2}{\sin^2 x} u_i \,, \tag{7.3}$$

with

$$(\partial_x^2 u)_i = \sum_{j,k\geq 0}^{N} (B'')_{ij} (B^{-1})_{jk} u_k \,, \tag{7.4}$$

where $(B'')_{ij} = \partial_x^2 e_j(x)|_{x_i}$ and $(B)_{ij} = e_j(x_i)$. These preparations transform the PDE (7.1) into an ODE system, which can be solved numerically. For the initial data we write

$$\begin{aligned} u(t,x)|_{t=0} =& \varepsilon \sum_{l\geq 0} \left(\alpha_l(0) + \bar{\alpha}_l(0)\right) e_l(x) \,, & (7.5)\\ =& \sum_{l\geq 0} f_l e_l(x) \,, & (7.6)\\ \partial_t u(t,x)|_{t=0} =& \varepsilon \sum_{l\geq 0} i\omega_l \left(\alpha_l(0) - \bar{\alpha}_l(0)\right) e_l(x) \,, & (7.7)\\ =& \sum_{l\geq 0} p_l e_l(x) \,, & (7.8) \end{aligned}$$

c.f. (5.3). Therefore we get

$$\begin{aligned} \alpha_l(0) =& \frac{1}{2\varepsilon} \int_0^\pi \left(u(0,x) - \frac{i}{\omega_l} \partial_t u(0,x) \right) e_l(x) & (7.9)\\ =& \frac{1}{2\varepsilon} \left(f_l - \frac{i}{\omega_l} p_l \right) \,, & (7.10) \end{aligned}$$

and for two mode initial data $\alpha(0) = \frac{1}{2}(1, 1/2, 0, ...)$

$$u(t, x_i)|_{t=0} = \varepsilon \left(e_0(x_i) + \frac{1}{2} e_1(x_i) \right) , \tag{7.11}$$

$$\partial_t u(t, x_i)|_{t=0} = 0 . \tag{7.12}$$

We integrate the system of ODE using Mathematica's *NDSolve*. Now to compare this solution with the resonant system we will compare the coefficients $c_j(t)$ from (5.3), i.e.

$$c_j(t) = \sum_{i \geq 0}^{N} (B^{-1})_{ji} u_i(t) , \tag{7.13}$$

for the PDE solution.

7.2 Numerical evolution of the resonant system

We truncate our system to 64-modes

$$2i\omega_n \frac{d\alpha_n}{d\tau} = \sum_{\substack{jlm \\ j+l=m+n}}^{64} S_{jlmn} \alpha_j \alpha_l \bar{\alpha}_m , \tag{7.14}$$

and solve it using fourth order Runge-Kutta method. The coefficients calculated from the resonant system are given by

$$\tilde{c}_j(t) = \varepsilon \left(\alpha_j(\varepsilon^2 t) e^{i\omega_j t} + \bar{\alpha}_j(\varepsilon^2 t) e^{-i\omega_j t} \right) . \tag{7.15}$$

We conclude from Fig 7.2.0 that the truncated resonant system (7.14) derived in Sec. 5 is a valid approximation for the PDE solution in timescales t/ε^2. As $\varepsilon \to 0$ the resonant system solution converges to the PDE solution. But due to the scaling property (5.58) we can conclude about the behaviour of solutions in the limit $\varepsilon \to 0$, making numerical calculations very cost efficient. Hence the resonant system approximates the PDE solution sufficiently.

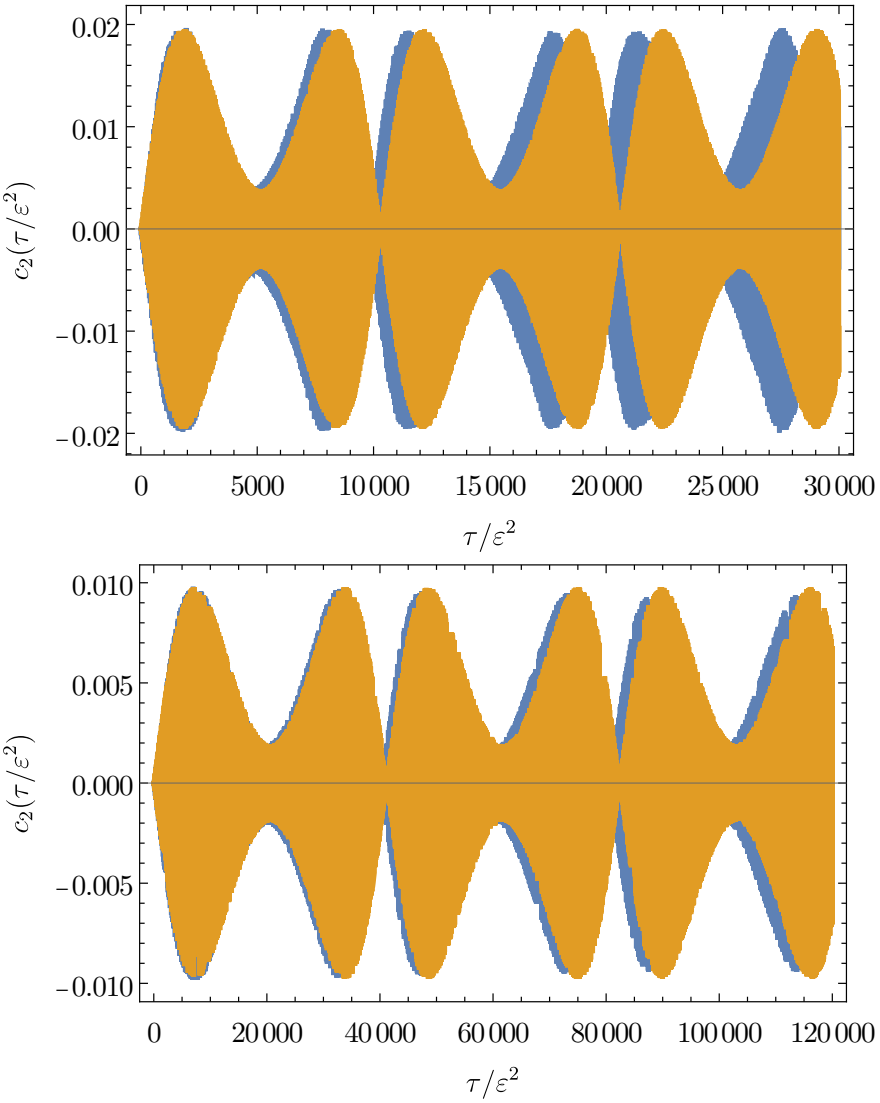

Figure 7.2.0: Evolution of the second mode of the truncated resonant system (blue) and the PDE solution (orange) with two mode initial data. *Top panel.* Size of perturbation $\varepsilon = 0.1$. *Bottom panel.* Size of perturbation $\varepsilon = 0.05$. The resonant system approaches the PDE solution as $\varepsilon \to 0$.

Chapter 8

Dynamics of the resonant system

In this section, we will study the dynamics of the resonant system that we derived in Sec. 5.5. We will start with the simplest form of initial data, that is, one-mode initial data. Since single-mode initial data remains stationary, we proceed with two-mode initial data leading to non-trivial evolution. While initially only the lowest-two modes are excited, the resonant system (5.57) induces energy transfer to higher-n modes. The evolution of two-mode initial data suggest that the solutions stay on an invariant manifold as in [22]. We then solve the equations describing the dynamics on this invariant manifold explicitly and show that the motion on the invariant manifold is periodic and the range of motion is bounded for all solutions within this ansatz. In the end we will look at perturbed two mode initial data and generic initial data, and numerically compute their solutions for long times.

8.1 One-mode initial data

The resonant system (5.55) admits solutions of the form

$$\alpha_n(\tau) = A_n e^{-i\lambda_n \tau}\,, \tag{8.1}$$

with time-independent frequencies $\lambda_n = \lambda - n\Omega$ and coefficients A_n for some real λ and Ω. These solutions we call stationary states, because there is no energy transfer between the modes. Inserting (8.45) into (5.55) we get the following nonlinear 'eigenvalue' problem

$$\omega_n(\lambda - n\Omega)A_n = \sum_{ijk}^{++-} S_{ijkn} A_i A_j \bar{A}_k\,. \tag{8.2}$$

The simplest solutions of this algebraic system are the one-mode stationary states with $\Omega = 0$

$$\alpha_n(\tau) = c\delta_{Nn} e^{-i\frac{S_{NNNN}}{\omega_N}|c|^2\tau}\,, \tag{8.3}$$

for any non-negative integer N, $c \in \mathbb{C}$. Hence solutions with one-mode initial data, such as

$$\alpha_n(0) = (1, 0, 0, 0, 0, ...)^T\,, \tag{8.4}$$

remain stationary as the solutions in (8.3) do not allow energy transfer between the modes.

8.2 Three-dimensional invariant manifold

In this chapter we give a similar analysis of the resonant system (5.55) as in [1]. Although, the interaction coefficients of the resonant system given in (8.26) does not fulfill the symmetry assumptions made in [1], we are still able to derive a three dimensional invariant subspace with remarkable properties.

8.2.1 Derivation

In [1] the authors have found a class of resonant systems, which all arise from cubic non-linearity. Such systems all admit a perfectly resonant spectrum and are of the form

$$i\frac{\mathrm{d}\beta_n}{\mathrm{d}\tau} = \sum_{mkl}^{++-} C_{nmkl}\beta_k\beta_l\bar{\beta}_m = \sum_{m=0}^{\infty}\sum_{k=0}^{n+m} C_{nmk,n+m-k}\bar{\beta}_m\beta_k\beta_{n+m-k}\,, \tag{8.5}$$

with $C_{0000} = 1$. The coefficients are symmetric under simultaneous perturbation $(n \leftrightarrow m), (k \leftrightarrow l)$ and under pair interchange $(n, m) \leftrightarrow (k, l)$. These infinite-dimensional Hamiltonian systems admit special analytic solutions and a complex conserved quantity. Following their work [1] we will bring (5.57) into the same form as (8.5) by the substitution $\alpha_l = \beta_l/\sqrt{\omega_l}$, the redefinition of interaction coefficients

$$C_{nmkl} = \frac{S_{nmkl}}{\sqrt{\omega_n\omega_m\omega_k\omega_l}}\frac{\omega_0^2}{S_{0000}}\,, \quad S_{0000} = -\frac{40}{3\pi}\,, \tag{8.6}$$

and a suitable rescaling of time $\tau \to \tau\frac{S_{0000}}{2\omega_0^2}$.

Similar to [1] we find that

$$Z = \sum_{n\geq 0}\sqrt{(n+1)(n+G)}\bar{\beta}_{n+1}\beta_n\,, \quad G = 4\,, \tag{8.7}$$

is a conserved quantity. The conservation can be shown numerically as seen in Fig. 8.2.0.

Motivated by [1, 22] and the evolution of two-mode initial data, see Fig. 8.2.1. We propose that the solution stays on an invariant manifold of the form

$$\beta_n(\tau) = f_n\left(b(\tau) + na(\tau)\right)p(\tau)^n\,, \quad f_n = \sqrt{\frac{(n+1)(n+2)(n+3)}{6}}\,, \tag{8.8}$$

Note that for $p \to 0$ with b and $(a-b)p$ finite, two mode initial data is included in the ansatz (8.8). Thus, in the language of [1] our system is of the $G = 4$, $\gamma = 5/8$ class/type. Following [1] we introduce the definitions

$$g_p^{(n,m)} = \sum_{k=0}^{n+m} k^p\frac{f_kf_{n+m-k}}{f_nf_m}C_{nmk,n+m-k}\,, \tag{8.9}$$

$$F_p(x) = \sum_{k=0}^{\infty} k^p f_k^2 x^k\,, \tag{8.10}$$

Performing the sums, we find that $g_p^{(n,m)}$ with $p = 0, 1, 2$ has to satisfy

$$g_0^{(n,m)} = 1\,, \tag{8.11}$$

$$g_1^{(n,m)} = \frac{1}{5}\left(n + 4m\right)\,, \tag{8.12}$$

$$g_2^{(n,m)} = \frac{1}{25}\left(n^2 + 16m^2 + 4(n+m) + 10nm\right)\,, \tag{8.13}$$

to give closure to the ansatz (8.8). $F_p(x)$ is then given by

$$F_p(x) = \left(x\frac{\mathrm{d}}{\mathrm{d}x}\right)^p\frac{1}{(1-x)^G}\,, \quad G = 4\,, \tag{8.14}$$

cf. [1]. Inserting (8.8) into (8.5) we get

$$i\left(\dot{b} + \dot{a}n + (b+an)\,n\frac{\dot{p}}{p}\right) = \sum_{j=0}^{\infty} f_j^2x^j(\bar{b} + \bar{a}j)\sum_{k=0}^{n+j}\frac{f_kf_{n+j-k}}{f_nf_j}C_{njk,n+j-k}(b+ak)(b+a(n+j-k))\,, \tag{8.15}$$

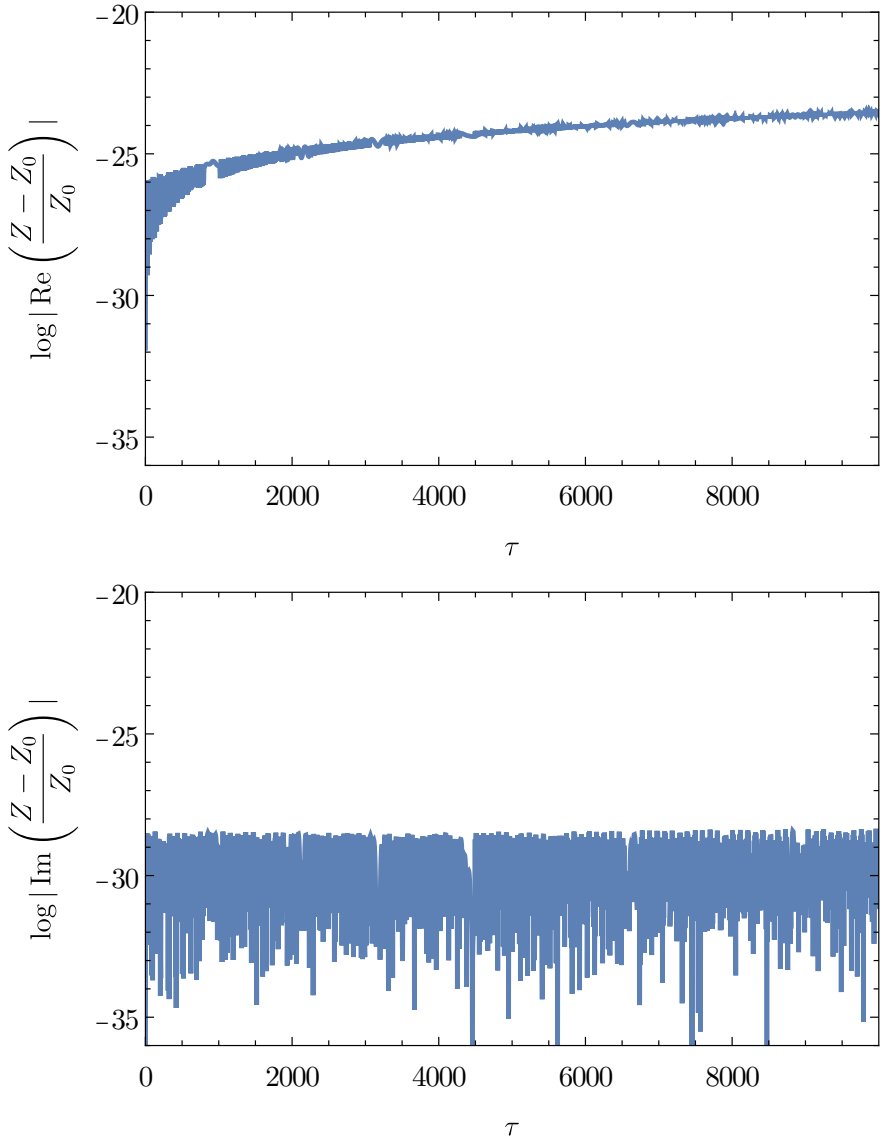

Figure 8.2.0: Evolution of the conserved quantity Z for two mode initial data truncated to 64 modes. *Top panel*. The real part of the relative error $\frac{Z-Z_0}{Z_0}$. *Bottom panel*. The imaginary part of the relative error $\frac{Z-Z_0}{Z_0}$. We conclude that Z is conserved over the course of simulation.

where $x = |p|^2$ and dot denotes differentiation with respect to τ. In terms of $g_p^{(n,m)}$ this yields

$$i\left(\dot{b} + \dot{a}n + (b + an)\, n\frac{\dot{p}}{p}\right) = \sum_{j=0}^{\infty} f_j^2 x^j (\bar{b} + \bar{a}j)\left(-a^2 g_2^{(n,m)} + a^2 g_1^{(n,m)}(j+n) + b g_0^{(n,m)}(a(j+n)+b)\right). \quad (8.16)$$

By the definitions (8.11)-(8.13), the RHS of (8.16) is a quadratic polynomial in n and m. Performing the summation over j using (8.10) and (8.14), transforms the RHS into a quadratic polynomial in n. The LHS is a quadratic polynomial in n as well. Comparing the coefficient of both polynomials we get three ordinary differential equations for the functions a, b and p. The

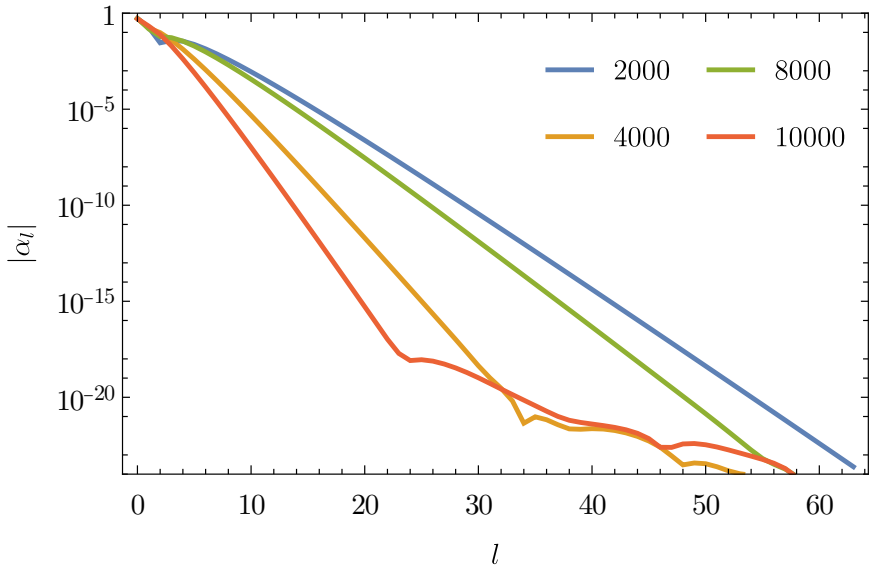

Figure 8.2.1: Mode amplitude spectrum for two-mode initial data truncated to 64 modes. The slope of the amplitude spectra is oscillating and showing turbulent behaviour. This oscillating behaviour is indicating stability of two-mode initial data. The kinks are due to truncation of the resonant system to 64 modes. They do not reflect the true dynamics of the system [69].

ansatz (8.8) is indeed preserved by (8.5) if the following differential equations are satisfied

$$i\dot{a} = \frac{4a^2\left(x(64x+11)\bar{a}+(-16x^2+17x-1)\,\bar{b}\right)}{25(x-1)^6} - \frac{21ab\left(4x\bar{a}-(x-1)\bar{b}\right)}{25(x-1)^5}\,, \tag{8.17}$$

$$i\dot{b} = -\frac{16a^2x^2\left((4x+2)\bar{a}-(x-1)\bar{b}\right)}{5(x-1)^7} + \frac{5b^2\left(4x\bar{a}-(x-1)\bar{b}\right)}{5(x-1)^5} \tag{8.18}$$

$$-\frac{20abx\left((4x+1)\bar{a}-(x-1)\bar{b}\right)}{5(x-1)^6}\,, \tag{8.19}$$

$$i\dot{p} = -\frac{4ap\left(4x\bar{a}-(x-1)\bar{b}\right)}{25(x-1)^5}\,, \tag{8.20}$$

Using the ansatz (8.8) and performing the sums in (6.1)-(6.3), the conserved quantities can be expressed in terms of a, b and p as follows:

$$\tilde{J} = \frac{-8(x-1)x\,\mathrm{Re}\left(a\bar{b}\right)+4x(4x+1)|a|^2+(x-1)^2|b|^2}{(x-1)^6}\,, \tag{8.21}$$

$$N = -\frac{4x\left((x-1)\left((x-1)|b|^2-2\left(4x\,\mathrm{Re}\left(a\bar{b}\right)+\mathrm{Re}\left(a\bar{b}\right)\right)\right)+\left(16x^2+13x+1\right)|a|^2\right)}{(x-1)^7}\,, \tag{8.22}$$

$$\begin{aligned}\widetilde{H} = \frac{1}{5(x-1)^{12}}\Big[&16a^2x^2\left(10\left(-4x^2+3x+1\right)\bar{a}\bar{b}+\left(80x^2+40x+3\right)\bar{a}^2+5(x-1)^2\bar{b}^2\right)\\ &+5b^2(x-1)^2\left((x-1)\bar{b}-4x\bar{a}\right)^2\\ &-40ab(x-1)x\left(\left(-8x^2+7x+1\right)\bar{a}\bar{b}+4x(4x+1)\bar{a}^2+(x-1)^2\bar{b}^2\right)\Big]\,,\end{aligned} \tag{8.23}$$

$$Z = -\frac{4\bar{p}\left((x-1)\left(-b(4x+1)\bar{a}-5ax\bar{b}+(x-1)|b|^2\right)+10x(2x+1)|a|^2\right)}{(x-1)^7}\,, \tag{8.24}$$

Note the following relation

$$\widetilde{H} = \tilde{J}^2 - S^2\,, \tag{8.25}$$

where

$$S = 4\sqrt{\frac{2}{5}}\frac{x}{(x-1)^6}|a|^2\,, \tag{8.26}$$

The conserved quantities (8.21)-(8.23) can be related to the conserved quantities defined in (6.1)-(6.3) by

$$\widetilde{J} = \sum_n |\beta_n|^2 = J\,, \tag{8.27}$$

$$N = \sum_n n|\beta_n|^2 = E - J\,, \tag{8.28}$$

$$\widetilde{H} = \sum_{\substack{jlmn \\ j+l=m+n}} \frac{\omega_0^2}{S_{0000}} S_{jlmn}\beta_j\beta_l\bar{\beta}_m\bar{\beta}_n = \frac{\omega_0^2}{S_{0000}}H \tag{8.29}$$

The conservation of Z can be verified by (8.17)-(8.20) but we make no claim about the conservation of (8.7) outside of the ansatz (8.8). The system (8.17)-(8.20) can be solved explicitly using the conservation laws. For our purposes we will limit ourselves to the inspection of x from which we can conclude the behaviour of the spectrum $|\beta_n|^2$.

8.2.2 Periodic motion on the invariant manifold

In the following we analyse the motion on the invariant manifold (8.8). Hence we show that x is periodic in time and therefore the spectrum $|\beta_n|^2$. First we start off by expressing $|a|^2$, $|b|^2$ and $\mathrm{Re}(a\bar{b})$ as functions of the conserved quantities. From (8.26) we get an expression for $|a|^2$ and therefore for the other two quantities

$$|a|^2 = \frac{\sqrt{\frac{5}{2}}S(x-1)^6}{4x}\,, \tag{8.30}$$

$$|b|^2 = \frac{1}{2}(x-1)^4\left(2N(x-1) + J(8x+2) + 5\sqrt{10}Sx\right)\,, \tag{8.31}$$

$$\mathrm{Re}\left(a\bar{b}\right) = \frac{(x-1)^5\left(2N(x-1) + 8Jx + \sqrt{10}S(9x+1)\right)}{16x}\,. \tag{8.32}$$

The equation (8.20) can be used to get an evolution for $\dot{x}$

$$\frac{\dot{x}}{x} = \frac{8}{25(x-1)^4}\,\mathrm{Im}(a\bar{b}) \tag{8.33}$$

Next, defining

$$y = \frac{x}{1-x} \tag{8.34}$$

and making use of $(\mathrm{Im}(ab))^2 = |a|^2|b|^2 - (\mathrm{Re}(ab))^2$, together with (8.30)-(8.32) one can express the square of $\dot{y}$ in terms of the conserved quantities

$$(\dot{y})^2 = \frac{-2N^2 + 2\sqrt{10}NS - 5S^2}{1250} + \frac{2}{625}y\left(4NJ + \sqrt{10}NS + 2\sqrt{10}JS - 25S^2\right) - \frac{2}{625}y^2\left(8J^2 + 25S^2\right)\,, \tag{8.35}$$

This equation is of the form of energy conservation for a one-dimensional harmonic oscillator with the solutions

$$y = A\sin\left(\Omega\tau + \varphi\right) + B\,, \quad \varphi = \mathrm{const}\,, \tag{8.36}$$

where we can read off the values of

$$\Omega = \frac{1}{25}\sqrt{16J^2 + 50S^2}\,, \tag{8.37}$$

$$A = \pm\frac{\sqrt{S\left(\sqrt{10}J - 5S\right)\left(2N^2 + 8NJ - 25S^2\right)}}{8J^2 + 25S^2}\,, \tag{8.38}$$

$$B = \frac{4NJ + \sqrt{10}NS + 2\sqrt{10}JS - 25S^2}{16J^2 + 50S^2}\,. \tag{8.39}$$

Therefore y is periodic, which transfers to x and hence β_n being periodic through (8.30)-(8.32) and

$$|\beta_n|^2 = f_n^2\left(|b|^2 + 2n\,\mathrm{Re}(\bar{a}b) + n^2|a|^2\right)x^n\,. \tag{8.40}$$

The solution y oscillates between y_+ and y_- given by $y_\pm = B \pm A$ and so we can conclude that the range of motion of y, described by $(1+y_+)/(1+y_-)$ is uniformly bounded for all solutions. To show this we write

$$\frac{1+y_+}{1+y_-} = \frac{(1+y_+)^2}{(1+y_+)(1+y_-)} \leq \frac{(1+y_+ + y_-)^2}{1+y_+ + y_- + y_+y_-}. \tag{8.41}$$

This form has the advantage that we can express $y_+ + y_-$ and y_+y_- directly through the coefficients of the polynomial (8.35) which is simpler than using the explicit expressions (8.37)-(8.39). More specifically

$$\begin{aligned}\frac{(1+y_+ + y_-)^2}{1+y_+ + y_- + y_+y_-} = \\ \frac{4(N+2J)^2\left(4J+\sqrt{10}S\right)^2}{(8J^2+25S^2)\left(2N^2+2N\left(8J+\sqrt{10}S\right)+32J^2+8\sqrt{10}JS+5S^2\right)} \\ \leq \frac{2(4J+\sqrt{10}S)^2}{8J^2+25S^2}\,.\end{aligned} \tag{8.42}$$

Since we have

$$J = \frac{|4xa-(x-1)b|^2}{(x-1)^6} + \sqrt{\frac{5}{2}}S \geq \sqrt{\frac{5}{2}}S\,, \tag{8.43}$$

it follows that

$$\frac{1+y_+}{1+y_-} \leq \frac{24}{5}\,. \tag{8.44}$$

This implies that for fixed y_- the maximum value of $|p|$ is bounded. Consequently solutions within the invariant manifold remain regular, and in particular any combination of two lowest mode initial data. In contrast, if p was not bounded and therefore $x \to 1$, the decay of the spectrum 8.40 would decrease, indicating instability, as it was observed in [4]. A bound on x also means a bound on the Sobolev norms (4.33) from which stability follows.

8.2.3 Stationary states

As in Sec. 8.1 the resonant system (5.57) admits solutions of the form

$$\alpha_n(\tau) = A_n e^{-i\lambda_n\tau}\,, \tag{8.45}$$

with time-independent frequencies $\lambda_n = \lambda - n\Omega$ and coefficients A_n for some real λ and Ω. We now consider these stationary states within the ansatz (8.8) where they take the form

$$b(\tau) = b(0)e^{-i\lambda\tau}, \quad a(\tau) = a(0)e^{-i\lambda\tau}, \quad p(\tau) = p(0)e^{-i\Omega\tau}\,. \tag{8.46}$$

Substituting this into the system (8.17)-(8.20), we can solve it explicitly. First we consider the case $a(0) = 0$. Here the solution is given by

$$b(t) = c \exp\left(-\frac{i|c|^2\tau}{(x-1)^4}\right), \tag{8.47}$$

and $p(t) = const$ and $x = |p|^2$. We plug this solution into (8.40) which leads to

$$|\alpha_n|^2 = \frac{f_n^2}{\omega_n}\left(|b(0)|^2\right) x^n \,. \tag{8.48}$$

For $x \to 0$ (two-mode-initial data) this yields an exponential decay as in Fig. 8.2.2. Therefore we observe that the solution (8.47) approaches the one-mode stationary solution, where only the zeroth mode is initially excited, asymptotically. Non-zero a and $\Omega = 0$ yields

$$b(0) = -4cx, \quad a(0) = (1-x)c, \quad \lambda = -\frac{12|c|^2 x}{5(x-1)^4}\,, \tag{8.49}$$

and therefore the spectrum behaves as

$$|\alpha_n|^2 \sim \frac{f_n^2}{\omega_n}\left(n^2|a(0)|^2 + \mathcal{O}(x) + \mathcal{O}(x^2)\right) x^n \,. \tag{8.50}$$

As we take $x \to 0$ the zeroth mode will not be excited in the solution (8.49), see Fig. 8.2.3.

In addition, x is restricted by the condition that $\kappa := \sqrt{x^2 - 22x + 1}$ should be real. Therefore for $x < x_* = 11 - 2\sqrt{30} \approx 0.0455$ there exists a pair of two-parameter families of stationary states with $\Omega \neq 0$ and $\mathrm{Re}\,(c) \neq 0$

$$a_\pm(0) = (1-x)c\,, \tag{8.51}$$

$$b_\pm(0) = -\frac{1}{2}c\left((9x+1) \pm \frac{\kappa}{\mathsf{sgn}(\mathrm{Re}(c))}\right), \tag{8.52}$$

$$\Omega_\pm = -\frac{2|c|^2}{25(x-1)^3}\left((x+1) \pm \frac{\kappa}{\mathsf{sgn}(\mathrm{Re}(c))}\right), \tag{8.53}$$

$$\lambda_\pm = \frac{|c|^2}{50(x-1)^3}\left(-\frac{(41x+25)\kappa\,\mathsf{sgn}(\mathrm{Re}(c))}{50(x-1)} \pm (25-41x)\right). \tag{8.54}$$

Inserting these solutions into the ansatz (8.8) yields the spectrum

$$|\alpha_n|^2 = \frac{f_n^2}{\omega_n}|c|^2\left(\frac{1}{4}(9x+1) \pm \kappa)^2 - n(1-x)((9x+1) \pm \kappa) + n^2(1-x)^2\right) x^n \,. \tag{8.55}$$

For $x \to 0, \kappa \to 1$ we get the following for the '$+$' solution in (8.51)-(8.54)

$$|\alpha_n|^2 \sim \frac{f_n^2}{\omega_n}\left(1 - 2n + n^2 + \mathcal{O}(x) + \mathcal{O}(x^2)\right) x^n \,. \tag{8.56}$$

Here we see that the decline at the first mode is due to $n = 1$ being the root of the polynomial $1 - 2n + n^2$, see Fig. 8.2.4. For the '$-$' solution the spectrum approximates to

$$|\alpha_n|^2 \sim \frac{f_n^2}{\omega_n}\left(n^2 + \mathcal{O}(x) + \mathcal{O}(x^2)\right) x^n \,. \tag{8.57}$$

Analogously to the nonzero a and $\Omega = 0$ case the zeroth mode will not be excited in this stationary solution as in Fig. 8.2.4. The x^n term dominates in all solutions for larger n leading to an exponential decay. The analytic solutions of the stationary states coincide with the data from the truncated resonant system, confirming the ansatz (8.8).

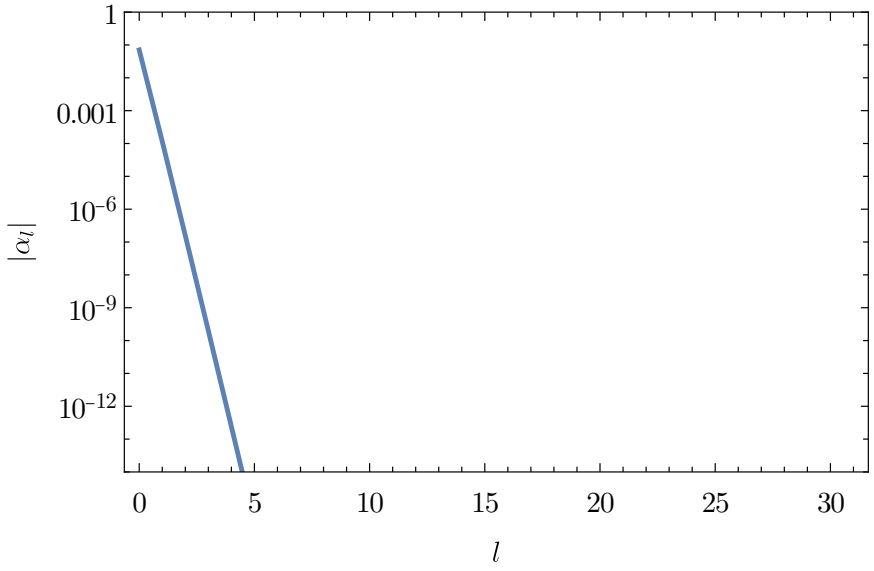

Figure 8.2.2: Mode amplitude of a stationary state with $a(0) = 0$ and $\Omega = 0$ showing exponential decay. The initial parameters are $p(0) = 0.001$ and $c = 0.1$.

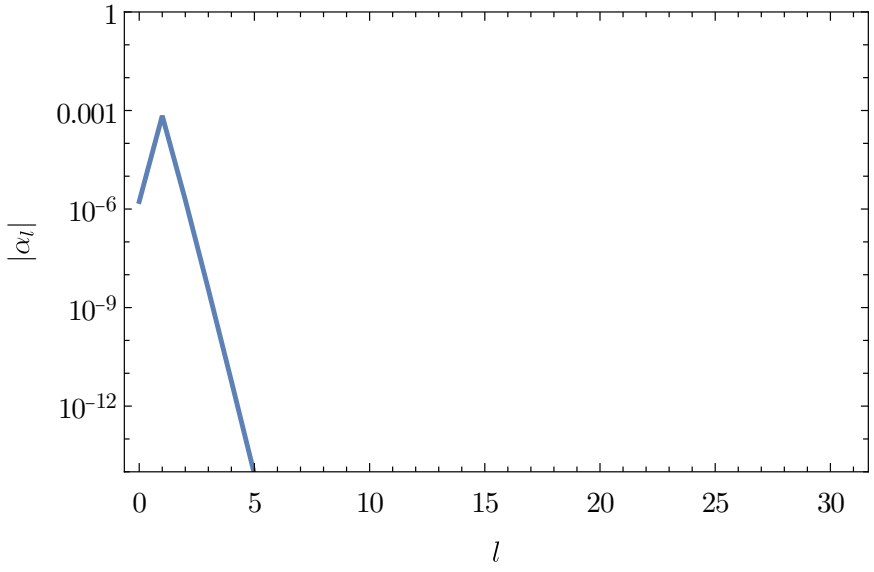

Figure 8.2.3: Mode amplitude of a stationary state with $a(0) \neq 0$ and $\Omega = 0$. The initial parameters are $p(0) = 0.001$ and $c = 0.6$

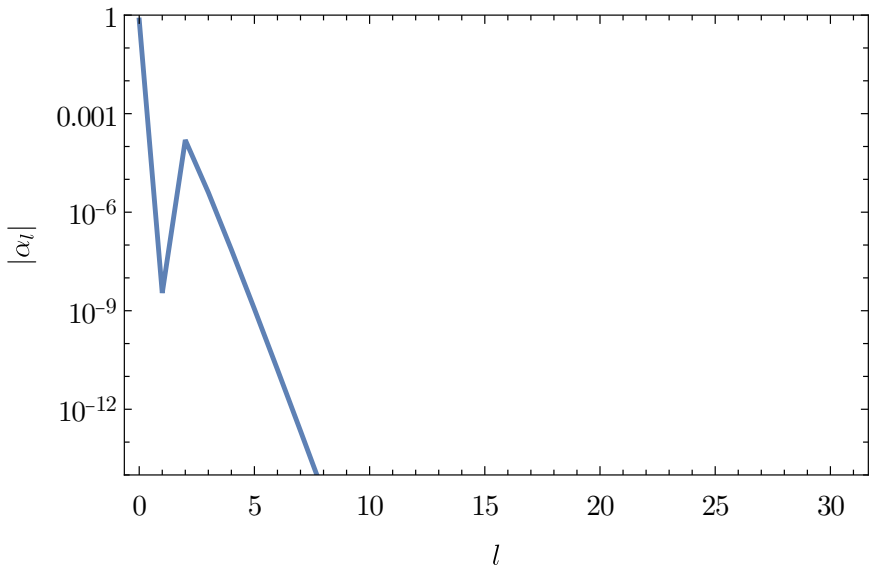

Figure 8.2.4: Mode amplitude of a stationary state of the '+' family of solutions with $a(0) \neq 0$ and $\Omega = 0$. The initial parameters are $p(0) = 0.01$ and $c = 1$.

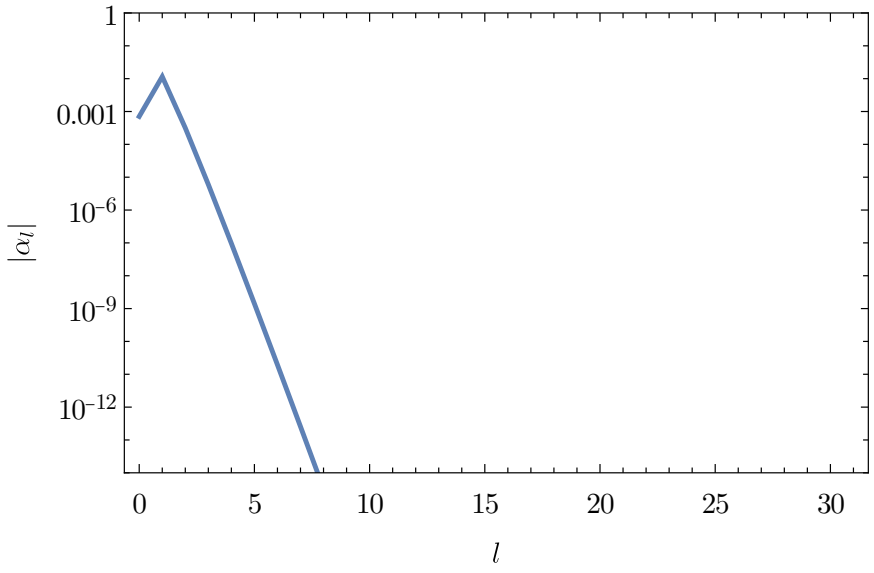

Figure 8.2.5: Mode amplitude of a stationary state of the '−' family of solutions with $a(0) \neq 0$ and $\Omega = 0$. The parameters are $p(0) = 0.01$ and $c = 1$

8.3 Three-mode initial data

After we were able to show analytically that the evolution of two-mode initial data stays bounded, it is only natural to consider three-mode initial data now. For this we choose the initial data to be of the form

$$\alpha_n(0) = \frac{1}{\sqrt{\omega_0^2(2+\delta^2)}}\left(1, \frac{\omega_0}{\omega_1}, \frac{\omega_0}{\omega_2}\delta, 0, ...\right) , \tag{8.58}$$

so that the total energy (6.2) does not change with different values of $\delta \in (0, 1)$. Numerical simulations show that the Sobolev norms (4.33), which are a measure of turbulent behaviour, i.e. energy transfer from lower l-modes to higher l-modes, are not bounded, except for $\delta < 0.44$ and $\delta > 0.8$ see Fig. 8.3.1. The Sobolev norms vary with different δ. Small δ corresponds to initial data with the lowest two modes excited and $\delta \to 1$ to initial data with the first and second mode excited. Therefore a small Sobolev norm for δ close to 0 and close to 1 is obvious from our analysis before. A maximum is reached at $\delta = 0.5$ and $\delta = 0.7$, c.f Fig. 8.3.2, however for $0.8 < \delta < 1$ the norms decrease again. Further numerical examination (longer times τ) of the $\delta = 0.7$ and $\delta = 0.8$ norms show that truncation to 64 modes was not enough and longer evolution is needed. The Sobolev norms Fig. 8.3.3 and mode amplitude spectrum for delta 0.7, we see that the norms seem saturated and the spectrum is equilibrating, see Fig. 8.3.5. For the $\delta = 0.8$ on the other hand, higher Sobolev norms are not bounded and the spectrum 8.3.4 is slowly increasing Fig. 8.3.6. The variation between different s norms indicates that energy is transferred from lower to higher frequencies and if the norms are saturated, the energy also flows back.

To conclude stability for three mode initial data, we would have to expand our numerical simulation to longer τ and higher l modes, and then confirm that also higher Sobolev norms are bounded for initial data with $0.44 \leq \delta \leq 0.8$. Because of our limitation to *Mathematica*, this cannot be done in a reasonable time.

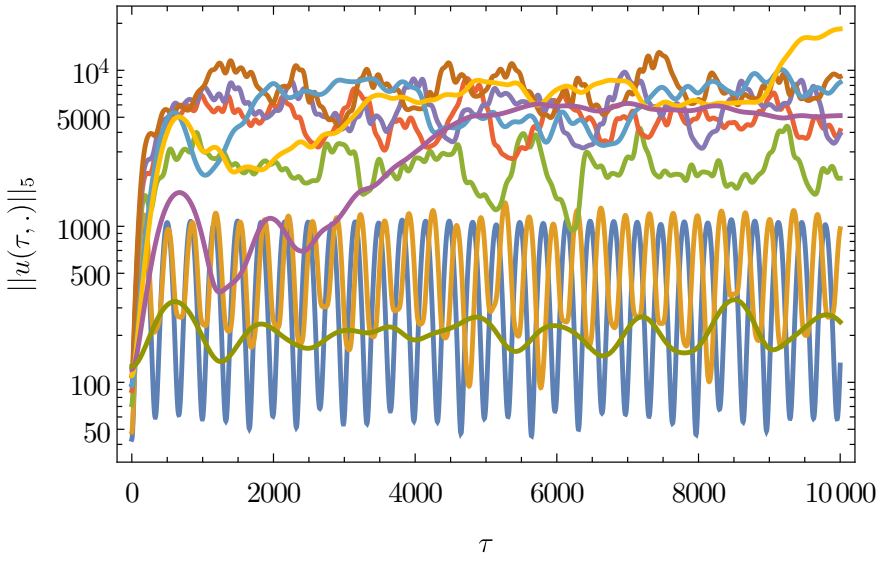

Figure 8.3.1: Evolution of Sobolev norms with $s = 5$ for three-mode initial data for a 64-mode truncated resonant system and with different initial data $\delta = 0.1$ (dark blue), 0.16 (dark orange), 0.33 (green), 0.41 (red), 0.44 (purple), 0.5 (brown), 0.6 (blue), 0.7 (yellow), 0.8 (lilac), 0.9 (dark green). We do not see saturation for $0.44 \leq \delta \leq 0.8$.

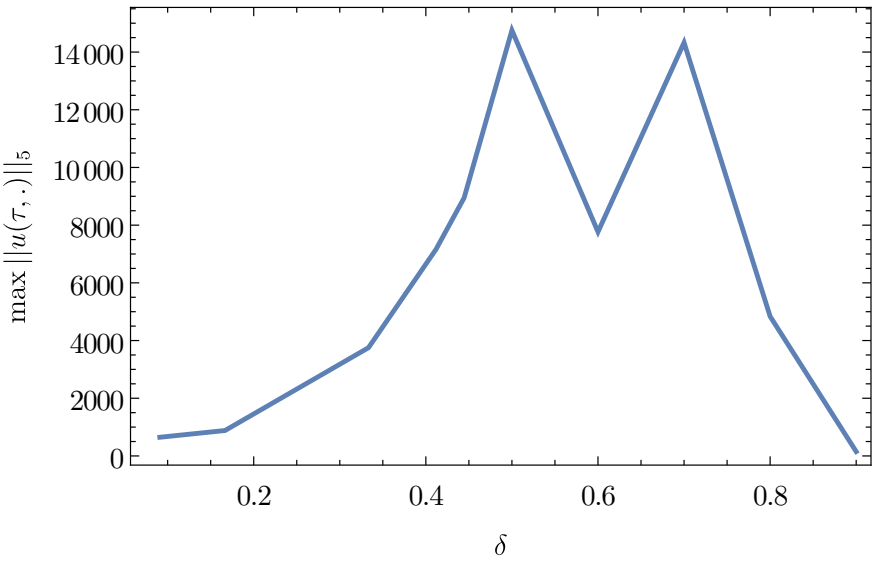

Figure 8.3.2: Maxima of $s = 5$ Sobolev norms for different perturbations of two-mode initial data. The Sobolev norm takes a minimum for two mode initial data. The most turbulent behaviour can be observed in the region $0.4 \leq \delta \leq 0.8$.

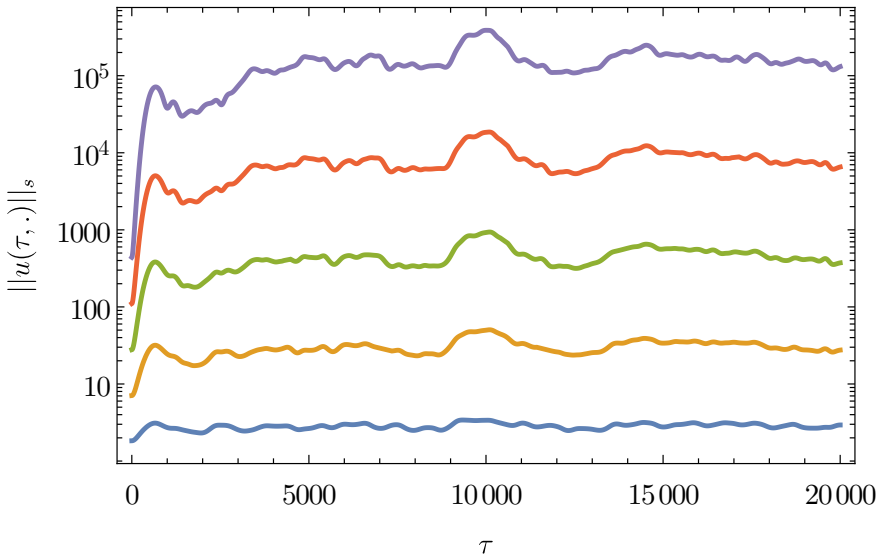

Figure 8.3.3: Sobolev norms with $s = 2, ..., 6$, with different line colors, from bottom to top and $\delta = 0.7$ initial data. We cannot conclude saturation for this initial data. Further examination is needed.

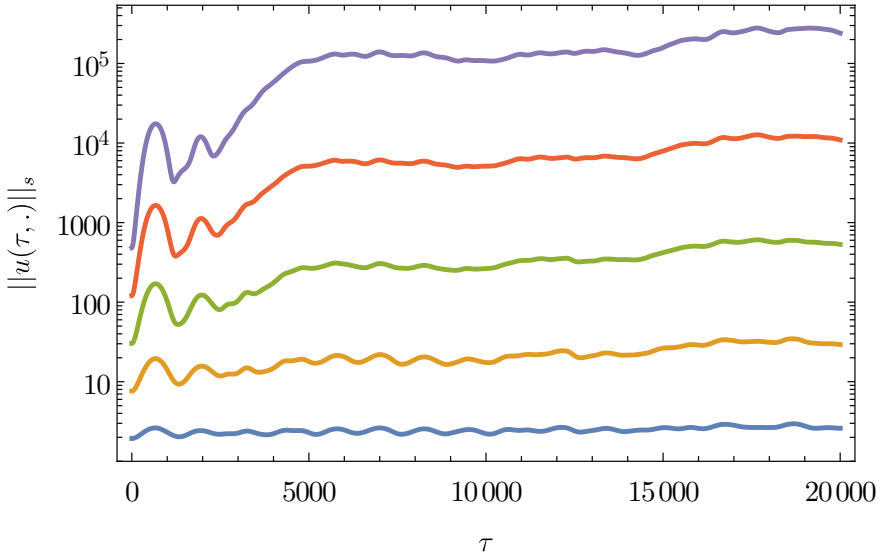

Figure 8.3.4: Sobolev norms with $s = 2, ..., 6$, with different line colors, from bottom to top and $\delta = 0.8$ initial data. Even though lower norms seem to be saturated, higher norms are not.

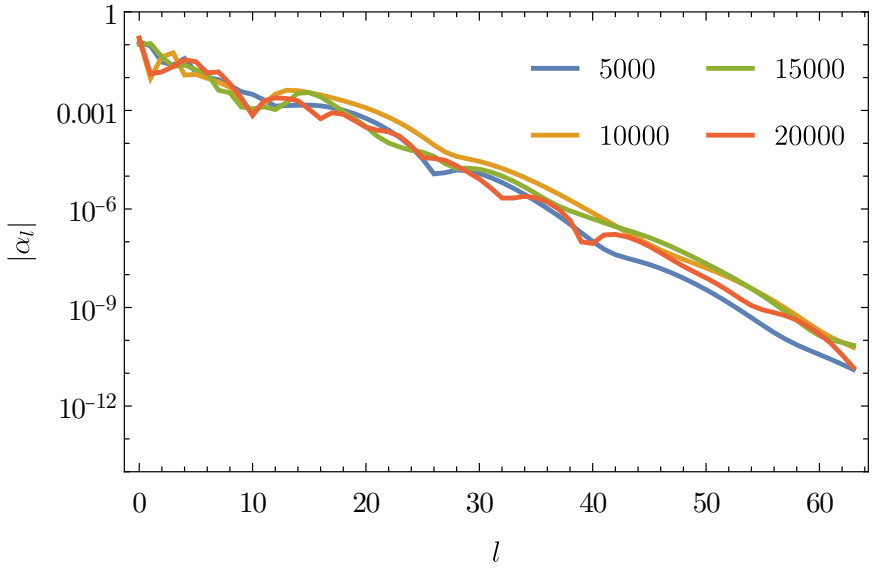

Figure 8.3.5: Evolution of the mode amplitude spectrum for $\delta = 0.7$ three-mode initial data. The spectrum equilibrates.

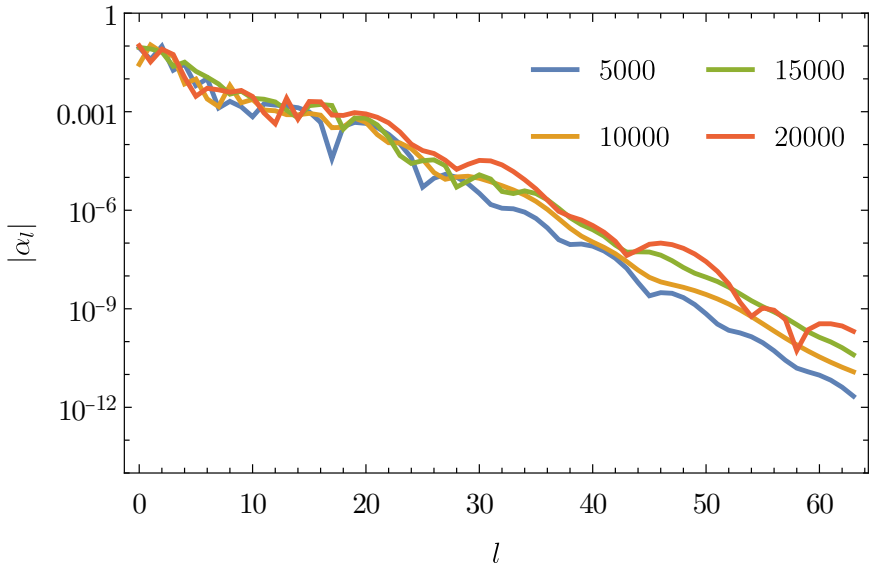

Figure 8.3.6: Evolution of the mode amplitude spectrum for $\delta = 0.8$ three-mode initial data. The spectrum grows with τ.

8.4 Generic initial data

We found that the solutions of the resonant system for two mode initial data are time-periodic. For three-mode initial data we were not able to conclude stability. To further examine the question of instability we consider a generic type of initial data and compare our results.

We therefore choose a Gaussian like localized distribution of the form

$$u(t,x)|_{t=0} = 0\,, \quad \partial_t u(t,x)|_{t=0} = \varepsilon \frac{\sin^2 x}{2} \exp\left(-4\sin^2\frac{x}{2}\right). \tag{8.59}$$

For the resonant system (5.57), we must bring this initial data into a compatible form. Evaluating the condition (8.59) with the ansatz (5.51) yields

$$u(t,x)|_{t=0} = \varepsilon \sum_{j\geq 0} \left(\alpha_j(0) + \bar{\alpha}_j(0)\right) e_j(x) = 0\,, \tag{8.60}$$

with eigenfunctions $e_j(x)$ defined in (4.28). From this we conclude that

$$\alpha_j(0) = -\bar{\alpha}_j(0)\,. \tag{8.61}$$

The other initial condition of (8.59) yields

$$\begin{aligned}\partial_t u(t,x)|_{t=0} =& \varepsilon \sum_{j\geq 0} i\omega_l \left(\alpha_j(0) - \bar{\alpha}_j(0)\right) e_j(x) \\ =& \varepsilon \sum_{j\geq 0} 2i\omega_l \alpha_j(0) e_j(x)\,.\end{aligned} \tag{8.62}$$

Now the initial condition for the resonant system is give by

$$\begin{aligned}\alpha_j(0) =& \frac{1}{2i\omega_j}\int_0^\pi \partial_t u(0,x) e_j(x) dx \\ =& \frac{1}{2i\varepsilon\omega_j}\int_0^\pi \varepsilon \frac{\sin^2 x}{2} \exp\left(-4\sin^2\frac{x}{2}\right) e_j(x) dx\,.\end{aligned} \tag{8.63}$$

Numerical evolution of Sobolev norms (4.33) shows saturation of higher norms, see Fig. 8.4.1. The variation between different s norms indicates turbulent energy transfer from lower l-modes to higher l-modes and back, as was observed in [24]. This energy transfer is also noticed in the spectrum of the mode amplitude, see Fig. 8.4.2.

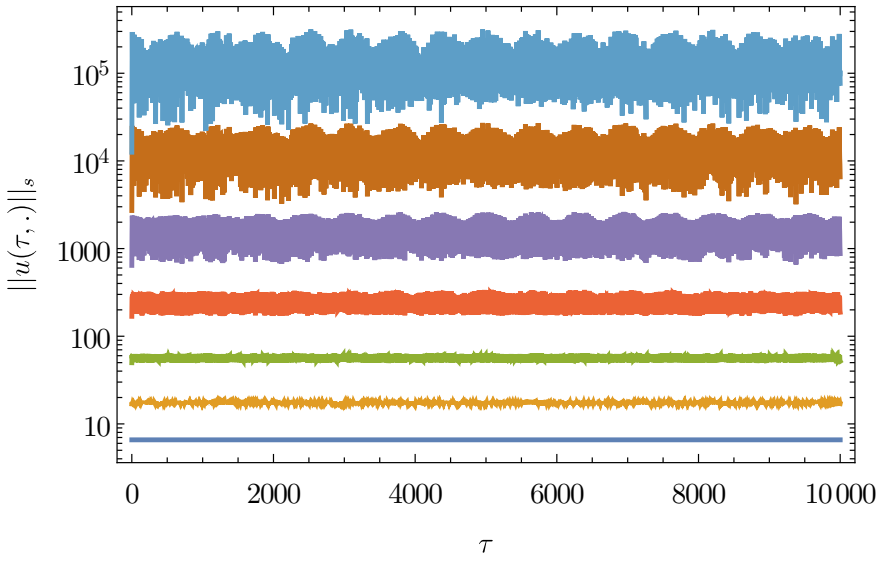

Figure 8.4.1: Sobolev norms with $s = 1, ..., 6$, with different line colors, from bottom to top for $\varepsilon = 100$ generic initial data. Higher Sobolev norms vary evidently from lower norms. This indicates energy flow from low l-modes to higher l-modes The $s = 1$ norm corresponds to the conserved quantity E.

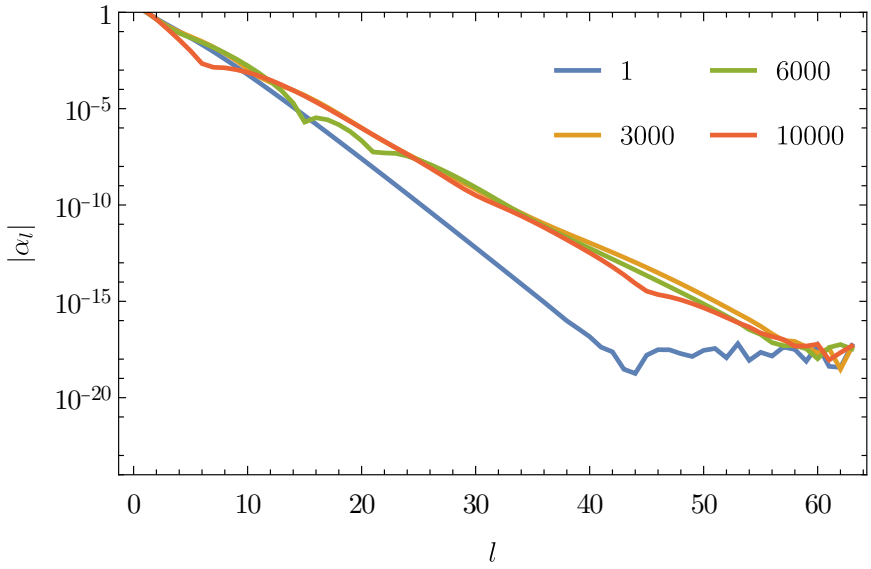

Figure 8.4.2: Evolution of the mode amplitude spectrum for generic initial data with $\varepsilon = 100$. The spectrum equilibrates.

Chapter 9

Summary and Conclusion

In this thesis we studied the dynamics of the Yang-Mills field on the Einstein Universe. Motivated by the instability of Anti-de Sitter spaces, we chose this toy model because of the conformal invariance of the Yang-Mills field in $3+1$ dimension and the conformal relation between AdS spacetime and the northern hemi-sphere of the Einstein universe $\mathbb{R} \times S^3$. We reviewed the last decades of research on AdS instability focusing on the conjecture by Bizoń and Rostworowski [4]. After stating basic definitions of general relativity, we gave an introduction to AdS spacetimes and the Einstein universe. We then derived the equations of motion of the Yang-Mills field and obtained a $1+1$ dimensional nonlinear PDE. This PDE admits two static solutions, each of them in a different topologically distinct sector. Because of the previous studies by Maliborski [24] we decided on perturbations around the static solution $S(x) = 1$ with a fully resonant linear spectrum. It has been shown [70] that an asymptotically resonant spectrum, as for the other solution $S(x) = \cos x$ is not strong enough to trigger turbulent behaviour and instability. Performing perturbative analysis of small solutions around the static solution we found secular terms, generated by nonlinearities. These secular terms falsify naïve perturbation theory, but can be removed introducing a 'slow' time, c.f. [17, 60, 71].

Repeating the perturbative analysis with two timescales, we obtained a coupled system of ODEs (resonant system) with a scaling property, that lets us conclude about the behaviour of arbitrarily small perturbations. We were able to find an explicit formula for the interaction coefficients of the resonant system. The system also admits symmetries from which we concluded three conserved quantities and showed their conservation analytically and numerically for two-mode initial data.

We showed that the resonant approximation does indeed give a good approximation to the nonlinear PDE and approaches the PDE solution as the size of the perturbation decreases. With the scaling property we can conclude about solutions with the same initial data in the limit $\epsilon \to 0$ from just calculating one solution.

Following the analysis of [1] we proposed that the resonant system admits a three-dimensional invariant manifold, on which the dynamics can be solved explicitly. These solutions show exact returns of the energy spectrum and their motion is bounded, i.e. the energy transfer from lower- to higher frequency modes cannot be made more turbulent by tuning initial conditions. The existence of time-periodic solutions is due to the lack of dissipation of energy [7]. In this analysis we have also found an additional complex valued conserved quantity and nontrivial stationary states.

To further examine the dynamics of our model we considered different kind of three-mode initial data. These solutions mostly showed saturated higher Sobolev norms and an equilibrated amplitude spectrum. The growth of the Sobolev norms lets us conclude to energy transfer from lower- to higher frequency modes. However some of the initial data has continuously increasing Sobolev norms and monotonically decreasing slopes of the amplitude spectrum. For this initial data and other data close to it, we have to extend our numerical calculations to longer times and more modes. Because of our restriction to *Mathematica* this cannot be done in a reasonable

times, but will be completed in the near future. To close our examination of the dynamics of the resonant system we considered generic initial data. We observed turbulent energy transfer, equilibrated energy spectrum and saturated Sobolev norms. In contrast to [13] we do not observe the typical behaviour for the evolution of the mode amplitude, that indicates instability.

For the future one can extend the numerical studies on three-mode initial data by choosing a faster programming language and making use of parallel computing. The search for more stationary states can be continued and their stability properties analysed.

We have derived the resonant system for the Yang-Mills field on a sphere and studied its dynamics. This toy model does not exhibit instability as Einstein-AdS, because the energy transfer stops at some point in time, in contrast to what has been observed in [13], and is therefore not the best model to consider. However non-linear partial differential equations on bounded domains have interesting non-trivial dynamics, such as turbulent behaviour, time-periodic and stationary solutions, and are worth investigating.

Bibliography

[1] A. Biasi, P. Bizoń, and O. Evnin, "Solvable cubic resonant systems," *Communications in Mathematical Physics*, vol. 369, no. 2, pp. 433–456, 2019.

[2] D. Christodoulou and S. Klainerman, *The Global Nonlinear Stability of the Minkowski Space (PMS-41)*. Princeton: Princeton University Press, 1994.

[3] H. Friedrich, "On the existence of n-geodesically complete or future complete solutions of Einstein's field equations with smooth asymptotic structure," *Communications in Mathematical Physics*, vol. 107, pp. 587–609, 1986.

[4] P. Bizoń and A. Rostworowski, "Weakly turbulent instability of anti–de sitter spacetime," *Phys. Rev. Lett.*, vol. 107, p. 031102, 2011.

[5] B. Craps, O. Evnin, and V. Luyten, "Maximally rotating waves in AdS and on spheres," *Journal of High Energy Physics*, vol. 2017, no. 9, 2017.

[6] P. Bizoń and A. Rostworowski, "Gravitational turbulent instability of AdS_5," *Acta Physica Polonica B*, vol. 48, no. 8, p. 1375, 2017.

[7] M. Maliborski and A. Rostworowski, "Time-periodic solutions in an Einstein AdS–massless-scalar-field system," *Physical Review Letters*, vol. 111, no. 5, 2013.

[8] J. Bičák, M. Scholtz, and P. Tod, "On asymptotically flat solutions of Einstein's equations periodic in time: I. vacuum and electrovacuum solutions," *Classical and Quantum Gravity*, vol. 27, no. 5, p. 055007, 2010.

[9] J. Bičák, M. Scholtz, and P. Tod, "On asymptotically flat solutions of Einstein's equations periodic in time: Ii. spacetimes with scalar-field sources," *Classical and Quantum Gravity*, vol. 27, no. 17, p. 175011, 2010.

[10] J. Maldacena, "The large-n limit of superconformal field theories and supergravity," *International Journal of Theoretical Physics*, vol. 38, no. 4, pp. 1113–1133, 1999.

[11] V. Balasubramanian, A. Buchel, S. R. Green, L. Lehner, and S. L. Liebling, "Holographic thermalization, stability of Anti–de Sitter space, and the Fermi-Pasta-Ulam Paradox," *Physical Review Letters*, vol. 113, no. 7, 2014.

[12] M. Maliborski, "Instability of flat space enclosed in a cavity," *Physical Review Letters*, vol. 109, no. 22, 2012.

[13] P. Bizoń , M. Maliborski, and A. Rostworowski, "Resonant dynamics and the instability of Anti–de Sitter spacetime," *Physical Review Letters*, vol. 115, no. 8, 2015.

[14] B. Craps, O. Evnin, and J. Vanhoof, "Renormalization group, secular term resummation and AdS (in)stability," *Journal of High Energy Physics*, vol. 2014, no. 10, 2014.

[15] B. Craps, O. Evnin, and J. Vanhoof, "Renormalization, averaging, conservation laws and AdS (in)stability," *Journal of High Energy Physics*, vol. 2015, no. 1, 2015.

[16] S. Kuksin and A. Maiocchi, "The effective equation method," in *New Approaches to Nonlinear Waves*, pp. 21–41, Springer International Publishing, 2016.

[17] C. Bender and S. Orszag, *Advanced Mathematical Methods for Scientists and Engineers: Asymptotic Methods and Perturbation Theory*, vol. 1. Springer, 1999.

[18] P. Bizon, D. Hunik-Kostyra, and D. E. Pelinovsky, "Stationary states of the cubic conformal flow on $\mathbb{S}^3$," 2018, 1807.00426.

[19] P. Gérard and S. Grellier, "The Szegö cubic equation," 2009, 0906.4540v1. `https://doi.org/10.48550/arXiv.0906.4540`.

[20] H. Xu, "Large-time blowup for a perturbation of the cubic Szegő equation," *Analysis &PDE*, vol. 7, no. 3, pp. 717–731, 2014.

[21] A. Biasi and O. Evnin, "Turbulent cascades in a truncation of the cubic Szegő equation and related systems," *Analysis & PDE*, vol. 15, no. 1, pp. 217–243, 2022.

[22] P. Bizoń, B. Craps, O. Evnin, D. Hunik, V. Luyten, and M. Maliborski, "Conformal Flow on S^3 and Weak Field Integrability in AdS_4," *Commun. Math. Phys.*, vol. 353, no. 3, pp. 1179–1199, 2017, 1608.07227.

[23] A. Biasi, P. Bizoń , B. Craps, and O. Evnin, "Two infinite families of resonant solutions for the Gross-Pitaevskii equation," *Physical Review E*, vol. 98, no. 3, 2018.

[24] M. Maliborski, "Dynamics of nonlinear waves on bounded domains," 2016, 1603.00935. `https://doi.org/10.48550/arXiv.1603.00935`.

[25] G. Gibbons, S. Hawking, G. Horowitz, and M. Perry, "Positive mass theorems for black holes," *Communications in Mathematical Physics*, vol. 88, pp. 295–308, 1983.

[26] R. Schon and S.-T. Yau, "Proof of the positive mass theorem. 2.," *Commun. Math. Phys.*, vol. 79, pp. 231–260, 1981.

[27] H. Lindblad and I. Rodnianski, "The global stability of Minkowski space-time in harmonic gauge," *Annals of Mathematics*, vol. 171, 2004.

[28] P. T. Chrusciel and E. Delay, "Existence of non-trivial, vacuum, asymptotically simple spacetimes," *Classical and Quantum Gravity*, vol. 19, no. 9, pp. L71–L79, 2002.

[29] D. Fajman, J. Joudioux, and J. Smulevici, "The stability of the Minkowski space for the Einstein–vlasov system," *Analysis & PDE*, vol. 14, pp. 425–531, 2021.

[30] L. Andersson and V. Moncrief, "Future complete vacuum spacetimes," 2003. `https://doi.org/10.48550/arXiv.gr-qc/0303045`.

[31] P. Breitenlohner and D. Z. Freedman, "Stability in gauged extended supergravity," *Annals of Physics*, vol. 144, no. 2, pp. 249–281, 1982.

[32] A. Ishibashi and R. M. Wald, "Dynamics in non-globally-hyperbolic static spacetimes: III. Anti-de Sitter spacetime," *Classical and Quantum Gravity*, vol. 21, no. 12, pp. 2981–3013, 2004.

[33] H. Friedrich, "Einstein equations and conformal structure: Existence of Anti-de Sitter-type space-times," *Journal of Geometry and Physics*, vol. 17, no. 2, pp. 125–184, 1995.

[34] M. T. Anderson, "On the uniqueness and global dynamics of AdS spacetimes," *Classical and Quantum Gravity*, vol. 23, no. 23, pp. 6935–6953, 2006.

[35] J. Jałmużna, A. Rostworowski, and P. Bizoń, "AdS collapse of a scalar field in higher dimensions," *Phys. Rev. D*, vol. 84, p. 085021, 2011.

[36] M. Bañados, C. Teitelboim, and J. Zanelli, "Black hole in three-dimensional spacetime," *Physical Review Letters*, vol. 69, no. 13, pp. 1849–1851, 1992.

[37] P. Bizoń and J. Jałmużna, "Globally regular instability of 3-dimensional Anti–De Sitter spacetime," *Physical Review Letters*, vol. 111, no. 4, 2013.

[38] A. Buchel, L. Lehner, and S. L. Liebling, "Scalar collapse in AdS spacetimes," *Physical Review D*, vol. 86, no. 12, 2012.

[39] A. Buchel, S. L. Liebling, and L. Lehner, "Boson stars in AdS spacetime," *Physical Review D*, vol. 87, no. 12, 2013.

[40] Ó . J. C. Dias, G. T. Horowitz, and J. E. Santos, "Gravitational turbulent instability of Anti-de Sitter space," *Classical and Quantum Gravity*, vol. 29, no. 19, p. 194002, 2012.

[41] Ó . J. C. Dias, G. T. Horowitz, D. Marolf, and J. E. Santos, "On the nonlinear stability of asymptotically Anti-de Sitter solutions," *Classical and Quantum Gravity*, vol. 29, no. 23, p. 235019, 2012.

[42] N. Deppe, "Resonant dynamics in higher dimensional Anti–de Sitter spacetime," *Phys. Rev. D*, vol. 100, p. 124028, 2019.

[43] Ó . J. C. Dias and J. E. Santos, "AdS nonlinear instability: moving beyond spherical symmetry," *Classical and Quantum Gravity*, vol. 33, no. 23, p. 23LT01, 2016.

[44] Ó . J. C. Dias and J. E. Santos, "AdS nonlinear instability: breaking spherical and axial symmetries," *Classical and Quantum Gravity*, vol. 35, no. 18, p. 185006, 2018.

[45] H. Bantilan, P. Figueras, M. Kunesch, and P. Romatschke, "Nonspherically symmetric collapse in asymptotically AdS spacetimes," *Physical Review Letters*, vol. 119, no. 19, 2017.

[46] M. W. Choptuik, Ó . J. Dias, J. E. Santos, and B. Way, "Collapse and nonlinear instability of AdS space with angular momentum," *Physical Review Letters*, vol. 119, no. 19, 2017.

[47] G. Moschidis, "A proof of the instability of AdS for the Einstein-null dust system with an inner mirror," *Analysis & PDE*, vol. 13, no. 6, pp. 1671 – 1754, 2020.

[48] G. Moschidis, "A proof of the instability of AdS for the Einstein-massless vlasov system," *Inventiones mathematicae*, vol. 231, pp. 1–206, 2022.

[49] P. Chruściel, *Elements of General Relativity*. Birkhäuser Cham, 2019.

[50] P. Bizoń, "Is AdS stable?," *General Relativity and Gravitation*, vol. 46, no. 5, 2014.

[51] J. B. Griffiths, *Exact space-times in Einstein's general relativity*. Cambridge monographs on mathematical physics, Cambridge: Cambridge Univ. Press, 1. publ. ed., 2009.

[52] S. M. Carroll, *Spacetime and Geometry: An Introduction to General Relativity*. Cambridge University Press, 2019.

[53] E. Witten, "Some exact multipseudoparticle solutions of classical Yang-Mills theory," *Phys. Rev. Lett.*, vol. 38, pp. 121–124, 1977.

[54] Y. Choquet-Bruhat, "Global solutions of Yang-Mills equations on anti-de Sitter spacetime," *Classical and Quantum Gravity*, vol. 6, no. 12, p. 1781, 1989.

[55] P. T. Chruściel and J. Shatah, "Global existence of solutions of the Yang–Mills equations on globally hyperbolic four dimensional Lorentzian manifolds," *Asian Journal of Mathematics*, vol. 1, no. 3, pp. 530–548, 1997.

[56] M. W. Choptuik, E. W. Hirschmann, and R. L. Marsa, "New critical behavior in Einstein-Yang-Mills collapse," *Physical Review D*, vol. 60, no. 12, 1999.

[57] G. Fodor and I. Rácz, "Numerical investigation of highly excited magnetic monopoles in $SU(2)$ Yang-Mills-Higgs theory," *Phys. Rev. D*, vol. 77, p. 025019, 2008.

[58] Y. Hosotani, "Exact solution to the Einstein-Yang-Mills equation," *Physics Letters B*, vol. 147, no. 1, pp. 44–46, 1984.

[59] J. Colliander, M. Keel, G. Staffilani, H. Takaoka, and T. Tao, "Weakly turbulent solutions for the cubic defocusing nonlinear Schrödinger equation," 2008, 0808.1742.

[60] D. Hunik-Kostyra and A. Rostworowski, "AdS instability: resonant system for gravitational perturbations of AdS_5 in the cohomogeneity-two biaxial Bianchi IX ansatz," *Journal of High Energy Physics*, vol. 2020, 2020.

[61] G. Szegö, *Orthogonal polynomials*. Colloquium publications / American Mathematical Society ; 23, reprint. with corrections ed., 2003.

[62] H. Chaggara and W. Koepf, "On linearization coefficients of jacobi polynomials," *Applied Mathematics Letters*, vol. 23, no. 5, pp. 609–614, 2010.

[63] The Wolfram Function Site. `http://functions.wolfram.com/05.06.17.0006.01`.

[64] J. A. Murdock, *Perturbations: Theory and Methods*. Society for Industrial and Applied Mathematics, 1999, https://epubs.siam.org/doi/pdf/10.1137/1.9781611971095.

[65] B. Craps and O. Evnin, "AdS (in)stability: an analytic approach," *Fortschritte der Physik*, vol. 64, no. 4-5, pp. 336–344, 2016.

[66] A. Buchel, S. R. Green, L. Lehner, and S. L. Liebling, "Conserved quantities and dual turbulent cascades in Anti–de Sitter spacetime," *Physical Review D*, vol. 91, no. 6, 2015.

[67] J. Shen, T. Tang, and Z. huan Teng, *Spectral and High-Order Methods with Applications*. Science Press, 2006.

[68] J. Boyd, "A numerical comparison of seven grids for polynomial interpolation on the interval," *Computers & Mathematics with Applications*, vol. 38, no. 3, pp. 35–50, 1999.

[69] A. Biasi, B. Craps, and O. Evnin, "Energy returns in global global AdS_4," *Physical Review D*, vol. 100, no. 2, 2019.

[70] M. Maliborski and A. Rostworowski, "What drives AdS spacetime unstable?," *Physical Review D*, vol. 89, no. 12, 2014.

[71] J. Kurzweil and M. Maliborski, "Resonant dynamics and the instability of the box Minkowski model," *Physical Review D*, vol. 106, no. 12, 2022.